DOI:10.14753/SE.2024.3008

SEMMELWEIS EGYETEM

DOKTORI ISKOLA

Ph.D. értekezések

3008.

HARGITAI DÓRA

Transzlációs vesekutatások és szervtranszplantáció
című program

Programvezető: Dr. Zsembery Ákos, egyetemi docens

Témavezető: Dr. Zsembery Ákos, egyetemi docens

DOI:10.14753/SE.2024.3008

CORRECTION OF IMPAIRED ANION SECRETION IN CFTR-RELATED CHRONIC PULMONARY DISEASES

PhD thesis

Dóra Hargitai

Semmelweis University Doctoral School

Theoretical and Translational Medicine Division

Supervisor: Ákos Zsembery MD, PhD

Official reviewers: Gábor Czirják MD, DSc
Petra Pallagi, PhD

Head of the Complex Examination Committee:

Alán Alpár MD, DSc

Members of the Complex Examination Committee:

László Cervenák, PhD
Mihály Kovács, DSc

Budapest

2024

DOI:10.14753/SE.2024.3008

Table of Contents

DOI:10.14753/SE.2024.3008

DOI:10.14753/SE.2024.3008

List of Abbreviations

$[Ca^{2+}]_i$ – intracellular calcium concentration

ABC – adenosine-triphosphate -binding cassette

ADOR – adenosine receptors

ADP – adenosine-diphosphate

ASL – airway surface liquid

ATP – adenosine-triphosphate

BSA – bovine serum albumin

BzATP – benzoylbenzoyl- adenosine-triphosphate

Ca^{2+} – calcium ion

CaCC – Ca^{2+}-activated chloride conductance

cAMP – cyclic adenosine monophosphate

cDNA – complementary deoxyribonucleic acid

CF – cystic fibrosis

CFTR – Cystic Fibrosis Transmembrane Conductance Regulator

Cl^- – chloride anion

COPD – chronic obstructive pulmonary disease

CSE – cigarette smoke exposure

Cu^{2+} – copper ion

DAPI – 4′,6-diamidino-2-phenylindole

EDTA – ethylenediaminetetraacetic acid

ENaC – epithelial sodium channel

FEV1 – forced expiratory volume in one second

FITC – fluorescein isothiocyanate

GABA – gamma-aminobutyric acid

HCO_3^- – bicarbonate anion

IP_3 – inositol-trisphosphate

K^+ – potassium ion

MCC – mucociliary clearance

ML – mucus layer

mRFP – monomeric red fluorescent protein

Na^+ – sodium ion

NAC/ACC – N-acetylcysteine

NBD – nucleotide-binding domain

Ni^{2+} – nickel ion

NMDA – N-methyl-D-aspartate

NMDG – N-methyl-d-glucamine

NPD – nasal potential difference

P2XR – P2X receptor

PAAG – polycationic bipolymer, poly (acetyl, arginyl) glucosamine

$PaCO_2$ – partial pressure of carbon dioxide in arterial blood

PBS – phosphate buffered saline

PL – periciliary layer

PLC – phospholipase C

PMCA – plasma membrane Ca^{2+} ATPase

R-domain – regulatory domain

ROI – regions of interest

S.E.M. – standard error of the mean

SOC – store-operated calcium channel

SPLUNC1 – short palate lung and nasal epithelial clone 1

TM – transmembrane domain

TMEM16 – transmembrane protein 16

UDP – uridine-diphosphate

UTP – uridine-monophosphate

WT – CFBE41o− cells were transfected with wild-type CFTR cDNA

Zn^{2+} – zinc ion

DOI:10.14753/SE.2024.3008

ZnR – zinc-sensing receptor

ΔF – CFBE41o− cells transfected with delF508 CFTR cDNA

DOI:10.14753/SE.2024.3008

1. Introduction

Cystic Fibrosis Transmembrane Conductance Regulator (CFTR) is a protein that is mainly localized on the apical surface of polarized epithelial cells in the body. It has been studied mostly in relation to cystic fibrosis (CF), a life shortening, severe inherited disease. The gene encoding the CFTR protein is located on chromosome 7 (7q31.2). It is approximately 250 kb, containing 27 exons. The encoded mRNA is approximately 6,5 kilobases long and is translated into a protein product of 1480-amino acids. CFTR protein belongs to the adenosine triphosphate (ATP)-binding cassette (ABC) transporter protein family and includes two transmembrane domains (TM1 and TM2), two cytosolic domains responsible for nucleotide-binding (NBD1 and NBD2) and a regulatory domain (R-domain). The R domain contains sites for protein kinase A and protein kinase C binding and is unique for CFTR in the ABC transporter family. The channel opens when its R-domain is phosphorylated in a cAMP-dependent manner by protein kinase A and the binding of ATP molecule results in the dimerization of the two NBDs, so chloride anion can cross the cell membrane. The hydrolysis of ATP triggers the closure of the channel, as this process separates the NBDs and the TMs conformation changes, so the exit of chloride anions is blocked [1].

1.1. Function of CFTR protein

Basically, anion channel function of CFTR is crucial in maintaining the osmotic balance and viscosity of the mucus in the airways, pancreas, intestine, salivary glands, liver, skin, reproductive organs (male and female). Composition of mucus in these organs is also altered by CFTR through its effects on other ion transporters, such as regulation of epithelial sodium channel (ENaC) and cooperativity with Cl^-/HCO_3^- transport. The latter plays an important role in the pH homeostasis of mucus, mainly in the airway surface liquid (ASL). In addition to Cl^- transport, the CFTR protein is also permeable to HCO_3^- [2]. Depending on the activity of other anion exchangers and transporters expressed on the basolateral membrane of epithelial cells, the CFTR protein can secrete HCO_3^- in the airways, intestine, pancreas, and salivary glands. HCO_3^- is important in controlling the pH of surface liquid layers on the surface of epithelial cells. CFTR likely controls ENaC by regulating local acid-base balance [3]. Prostasin, a membrane-anchored serine protease

with trypsin-like substrate specificity, likely is required to activate ENaC [4]. Another regulatory protein, short palate lung and nasal epithelial clone 1 (SPLUNC1) is unable to inhibit ENaC in acidified ASL. CFTR can also regulate other ion channels, such as the outwardly rectifying chloride channel, the Ca^{2+}-activated chloride conductance (CaCC), the renal outer medullary K^+ channels, the sodium/proton exchanger, and an aquaporin channel [5,6].

CFTR protein is also expressed by immune cells, such as macrophages and neutrophil granulocytes. Macrophages in CF show multiple defects, including ineffective uptake of pathogens and a decreased efferocytosis (removal of apoptotic cells by phagocytes), phagocytosis, reactive oxygen species production and bacterial killing [7]. Also CFTR influences the synthesis of lipids that are components of cell membranes. CFTR is also involved in the transport of glutathione and thiocyanate and maintains their physiological level in the airway liquid layer. They serve as natural antioxidants, especially in the lungs [1].

1.2. ASL

Airways are lined by a respiratory type of epithelium and approx. 10 μm thick liquid layer, called ASL [8]. ASL is produced by submucosal glands and transepithelial ion movements due to osmosis. It has two layers: the mucus layer (ML) and the periciliary layer (PL). The gel-forming mucins are in the ML to trap inhaled particles and pathogens. While the PL is in direct contact with epithelial cells, and made up mostly from water, containing salt and lipids. This layer helps the cilia to beat properly. Effective mucociliary clearance (MCC) depends on the thickness and composition of ASL, which is mainly regulated by two ion channels: CFTR and ENaC. CFTR secretes Cl^- at the apical surface of epithelial cells and downregulates ENaC to restrict Na^+ absorption. Because of its effect on HCO_3^- secretion, CFTR plays a crucial role in maintaining the ASL physiologic pH (~7.1) which is important to promote a competent innate immunity in the lung [8]. Effective MCC also depends on proper ciliary beat frequency. Failure or slow-down of ciliary beating results in chronic respiratory diseases. This is clearly illustrated by patients suffering from primary ciliary dyskinesia as they develop chronic airway inflammation and bronchiectasis in childhood. Modulation of ciliary beat frequency requires a number of independent regulatory mechanisms. Extracellular purines, β-agonists, cholinergic agonists, temperature and mechanical forces affect ciliary beating. One of the primary

mechanisms that increase ciliary beat frequency is the increase in intracellular calcium [9].

1.3. Cystic fibrosis: an inborn error of CFTR

More than 2000 mutations in the CFTR gene have been found to cause CF [10]. In CF the majority of mutations involve changes in three or fewer nucleotides resulting in amino acid substitution, splice sites, frame shifts or nonsense mutations. The most common mutation is ΔF508, which involves a three base pair deletion encoding a phenylalanine at position 508 of the CFTR protein. The frequency of other CFTR mutations is low, except for some rare alleles among specific ethnic groups. For example, the W1282X mutation, which is a stop codon, accounts for 48 % of CFTR mutations in Ashkenazi Jews. CF mutations can disrupt CFTR function through various mechanisms, ranging from complete abortion of protein synthesis to normal apical membrane expression of the protein with poor anion conductance. These mutations are grouped into 6 classes. In classes I. and II. the major fraction of CFTR protein does not reach the cell membrane. In classes III., IV., V., VI. the protein is expressed on the apical surface but with altered or impaired function: defective regulation (class III.), defective conductance (class IV.), partially defective production or processing (class V.) and reduced conductance of other ion than chloride (class VI.). The most common and first identified mutation is ΔF508, a three base pair deletion encoding a phenylalanine at the position 508 of the CFTR protein. This is a prototype of class II. mutation, where the deficient protein is misfolded, which leads to premature degradation by ubiquitin-proteosomal pathway. Therefore, the CFTR protein never reaches the apical surface of the cell except for special experimental conditions, such as low temperature. Mutations of class I.-III. result in reduced or non-functional CFTR and are associated with severe phenotypes. In mutations of class IV.-V. some residual CFTR-mediated channel function remains, so the disease is milder. However, most class VI mutations are considered to be severe [11.].

1.4. Pathophysiology of CF

In CF the morbidity and mortality is caused by airway destruction, characterized by a vicious cycle of obstruction, inflammation and infection leading to respiratory failure and

death. However, data shows steady gain of survival for patients with CF, in 2019 half of the deaths reported to the Cystic Fibrosis Registry occurred before the age of 32. So, people with CF still tend to die before they finish school, start a career or establish a family. Still, it is important to note that the median survival age of those born in 2016 is predicted to be 47,7 years of age. However, CF has a complex phenotype not merely affecting lungs but also GI tract, pancreas, liver, sweat glands and reproductive organs. In the intestine it causes meconium ileus (often the first sign before birth), distal intestinal obstruction syndrome and rectal prolapse. In the pancreas exocrine insufficiency and CF-related diabetes is detected. In the liver the thick secretum leads to obstructive biliary tract disease. The involvement of the reproductive tract is responsible for male and female infertility. The alteration of ion composition of the sweat is used for diagnosis, the sweat test. It is based on a symptom of CF that was first observed in medieval times and was believed to be a curse on a child by witches: "Woe to the child who tastes salty from a kiss on the brow, for he is cursed and soon will die." [12]. The sweat of CF patients contains chloride over 60 mmol/l, while the normal amount of chloride in the sweat is less than 29 mmol/l. Sweat test is simple and non-invasive: after a brief chemical and electrical stimulation of the skin, sweat is collected for 30 minutes and then sent to a laboratory for analysis [13]. Clinically, the typical CF is characterized by accumulation of dehydrated and hyperviscous mucus, which reduces mucociliary clearance and favors infection of the airways, leading to chronic inflammation and destruction of the tissue (Figure 1.). Structural changes in the lungs occur earlier than previously thought and can be detected shortly after the diagnosis in newborns with CF. Acute bacterial infections trigger recurrent exacerbations and chronic tissue destruction results in bronchiectasis. *Pseudomonas aeruginosa*, the most common pathogen in CF airways in adolescents and adults [14], is associated with acceleration of lung impairment and with poorer prognosis. First, hyperinflation of the lungs can be observed, while atelectasis, pneumothorax and hemoptysis are symptoms of more advanced stages.

As mentioned above, CFTR plays a crucial role in maintaining the ion composition of ASL in the lung. In CF, the loss of function of CFTR causes a defect in Cl^- secretion, and it also fails to inhibit ENaC, therefore intracellular Cl^- and Na+ concentrations are elevated, promoting water absorption through aquaporins. On the other hand, the interstitial NaCl retention induces water to leave ASL paracellularly [1]. ASL dehydration contributes to mucus hyperviscosity and restricts cilia function. The pH of ASL is also altered in CF, because of the impaired HCO_3^- secretion via CFTR (Figure 2.) [2]. There

is emerging evidence that CFTR's role as a HCO_3^- channel - a driver of chloride-bicarbonate exchange and also a pH modifier - may be the key to explain symptoms of CF. Decreased pH promotes bacterial colonization and makes innate immunity incompetent. Normal ASL has a pH around 7.0-7.1 (estimated HCO_3^- concentration is approximately 10-20 mM), while in CF pigs and newborns with CF, airway pH is lower than in controls [15, 16]. However, paracellular bicarbonate flow down its concentration gradient from the blood to the airways seems to limit the average difference between CF and control airways less than 0.5-unit in pH. It is possible that airway clearance is also affected by changes in pH: transient acidification of normal ASL increases rate of electrolyte and fluid absorption by epithelium, while transient alkalinization leads to slowing-down of hyperabsorption and restores the height of ASL [15]. Impaired mucociliary clearance can be only partially explained by dehydrated ASL and diminished ciliary function, it also seems to be related to increased mucus viscosity. Mucins in the airways are secreted by goblet cells. Mucin formation and release is a complex process: it has an intracellular phase of synthesis, packaging and apical granule exocytosis then it is followed by an extracellular phase of mucin swelling, transport and discharge to the lumen. Normal mucus production requires concurrent exocytosis of mucin granules and a CFTR-dependent bicarbonate secretion to enhance extracellular phases of mucus excretion. Yang et al have demonstrated that in CF intestine goblet cells exhibited exocytosis, but mucus discharge was compromised and incomplete even when stimulated in the presence of HCO_3^- [17]. Mucins are excreted in granules condensed by Ca^{2+} [18]. Normally bicarbonate promotes completed mucin expansion, so mucins are released in long strands. Without bicarbonate (in CF) mucins become tangled and sticky, due to impaired mucin expansion [19]. Mucins help trap microorganisms and submucosal glands also secrete defensins (antimicrobial proteins). Protection against microbes is crucial in airways because the epithelium is in direct contact with the outside world. As previously mentioned, colonization of lungs with *Pseudomonas aeruginosa* is associated with poorer prognosis in CF patients and has long been recognized as the hallmark of CF, although the exact causal relationship remains unclear. Various defensins function optimally at neutral or alkaline pH, while lower pH reduces their activity. Interestingly newborn CF piglets are unable to kill bacteria [16]. The pH of airway surface is lower in CF pigs than in wild-type controls suggesting that the sub-optimal functioning of defensins in an acidic environment is responsible for the lack of bacterial killing [18].

DOI:10.14753/SE.2024.3008

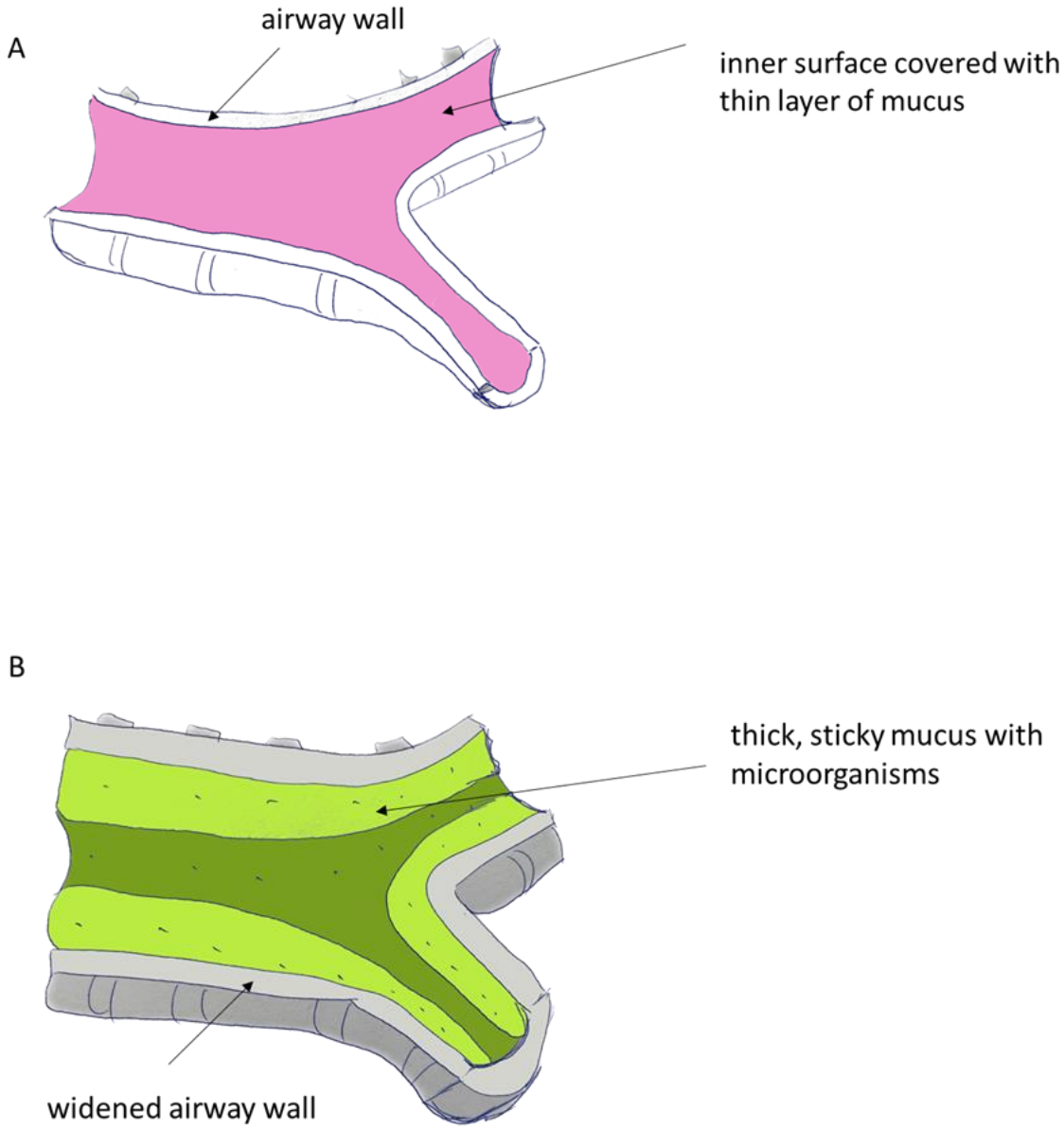

Figure 1. (A) Anatomy of a normal airway. (B) In CF airways the lumens are widened, and thick, sticky mucus covers the inner surface, which contains blood and microorganisms.

Based on the figure from https://www.nhlbi.nih.gov/health/cystic-fibrosis/symptoms

DOI:10.14753/SE.2024.3008

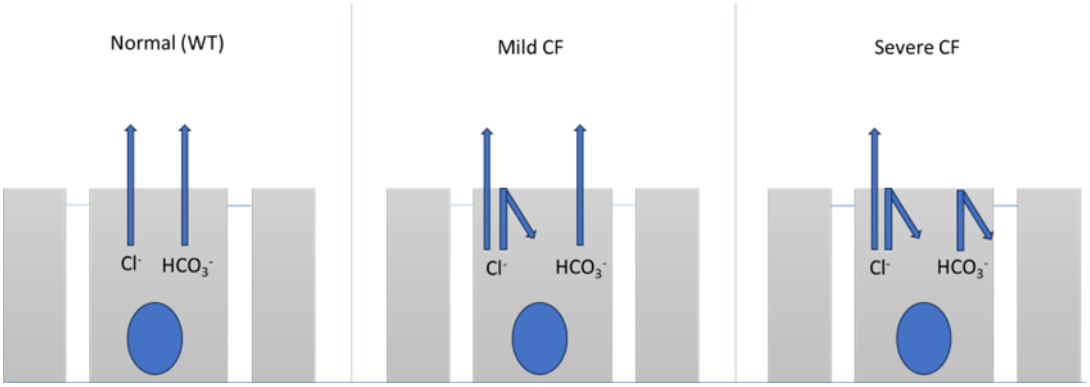

Figure 2. In normal airway bronchial epithelial cells secrete Cl^- and HCO_3^-. In mild CF due to the abortive function of CFTR Cl^- secretion is partially compromised. In severe CF both Cl^- and HCO_3^- are retained in the cells.
Based on the Figure of Quinton PM. The neglected ion: HCO_3^-. Nat Med. 2001 Mar;7(3):292-3.

1.5. COPD, an acquired dysfunction of CFTR

Chronic obstructive pulmonary disease (COPD) is a progressive respiratory disorder consisting of chronic bronchitis and/or emphysema and it is the third leading cause of death worldwide, that caused 3.23 million deaths in 2019. Environmental exposure to tobacco smoke, indoor air pollution and occupational dust, fumes and chemicals are important risk factors for COPD. Also, alpha-1-antitrypsin deficiency promotes COPD progression in smokers. Symptoms of COPD include breathlessness or breathing difficulty, chronic cough often with phlegm and tiredness. Approximately two-thirds of COPD patients have chronic bronchitis, characterized by excess mucin production and recurrent cough. This disease resembles the respiratory phenotype of CF including mucus accumulation, recurrent bacterial infections and persistent airway inflammation. The other main symptom of COPD is emphysema involving the destruction of the alveoli in the lungs. Thick mucus production is associated with mucus plugging, which obstructs the small airways, causing airflow limitation. Hypersecretion of mucus is the main cause of reducing FEV_1, which is a characteristic finding in COPD, leading to a poor quality of life, increased exacerbations, and increased risk of death. Currently, therapies for COPD focus primarily on symptom treatment and reduction of the frequency of acute

exacerbations. Mucus accumulation is mainly treated via nonpharmacological recommendations such as smoking cessation, physical exercise, and pulmonary rehabilitation because first-generation mucolytics were not sufficiently bioactive to alter outcomes [20, 21].

1.6. COPD pathophysiology

Inhaled tobacco smoke consists of gas and solid phases. The gas phase contains a high concentration of short-lived reactive intermediates (superoxide, hydrogen peroxide, nitric oxide). The reactive species in cigarette smoke are detoxified by antioxidants in the ASL. When antioxidants are depleted, these reactive species interact with biological targets on airway epithelium. The solid phase of gas contains a high concentration of free radicals such as semiquinones, hydroquinones and carbon-centered free radicals. This phase can produce large amounts of H_2O_2 in aqueous extracts and leads to production of hydroxyl radicals. Cigarette smoke and reactive intermediates have high inflammatory potential and promote the recruitment of inflammatory cells in the lungs [21].

1.7. COPD and ASL

Compromised mucociliary clearance is the central feature of respiratory pathology in COPD. Both the composition of ASL and efficient ciliary action are critical for cleansing the airways for maintaining normal respiratory function. A common feature of CF and COPD is that the height of PL is reduced in experimental models. Cantin et al. tested the effects of cigarette smoke exposure in human airway cells (Calu-3) and demonstrated that CFTR expression and function were decreased by cigarette smoke [22]. Using nasal potential difference (NPD) measurements, they demonstrated that healthy smokers without CFTR mutations displayed an NPD pattern similar to CFTR deficiency. They also suggested this could contribute to the pathophysiology of chronic bronchitis seen in cigarette smokers. Rowe et al. confirmed that CFTR dysfunction is present in cigarette smokers with and without COPD in the nasal airway and lung. Furthermore, in both the nose and lung, CFTR dysfunction was associated with chronic bronchitis, indicating the clinical relevance of the finding [23, 24]. Two independent research groups (Tarran and colleagues and Rowe and colleagues) demonstrated that cigarette smoke causes ASL

volume depletion and mucus dehydration due to loss of CFTR (because of internalization and transport to aggresome-like compartments) [25, 23]. It has been also shown that CFTR activity is reduced in smokers with COPD. Although the reduction is variable across individuals, a study using sweat ion measurements as a functional measure of systemic CFTR activity showed 40% decrease in CFTR activity in smokers and former smokers with COPD and 25% decrease in "healthy" smokers compared with non-smoker controls [26]. Studies suggest that both CFTR intrinsic functionality and expression at the cell surfaces of the airway lumen can be affected in COPD. Recent evidence from *in vitro* and *in vivo* animal studies, as well as primary human cell cultures, has shown that exposure to cigarette smoke reduces CFTR mRNA expression. Also, in primary human cell cultures cigarette exposure decreased CFTR protein expression to a greater extent than it did with mRNA expression, suggesting that protein degradation or depletion may play a greater role in CFTR dysfunction than diminished transcription [27]. Furthermore, several airway hypoxia models (human cell lines, *in vivo* animal experiments) decreased both CFTR mRNA and protein expression.

Airway mucin concentration is higher in current and former smokers with COPD. Loss and shortening of cilia may also contribute to the collapse of ASL and the impaired ability to remove foreign particles and pathogens from the airways. Elevated mucin concentration further contributes to PL dehydration through osmotic force, as water is drawn from PL to ML, enhancing mucus stasis. Severity of airway obstruction is directly linked to mucus plugging. Mucus plugs in the lower airways can lead to local hypoxia, which is likely to contribute to decrement of CFTR expression and function. Mucus accumulation favors bacterial colonization and results in neutrophilic inflammation. Constant chronic inflammation induces goblet cell hyperplasia and excess mucus production. Impaired mucociliary clearance results in pathogens and foreign particles being trapped in the airways, increasing the risk of infection and inflammation, which impairs cilia activity, closing the vicious circle. Increased neutrophil elastase activity is a component of the inflammatory response seen in chronic bronchitis, and *in vitro* and *in vivo* studies have demonstrated the ability of neutrophil elastase to degrade CFTR. Also, neutrophil activity can increase independent of infection, as a result of mucus accumulation, by "priming", when neutrophils are more readily activated to secrete proteases, increasing the potential of tissue destruction and CFTR protein degradation. Reduced CFTR function, just like in CF, results in decreased HCO_3^- secretion and reduction of ASL pH which further inhibits ciliary beating. *In vivo* and *in vitro* studies

demonstrated that cigarette smoke exposure leads to increased internalization of CFTR, Ca^{2+} release-induced inhibition and retrograde trafficking to endoplasmic reticulum. Cigarette smoke has a direct effect on CFTR by covalent modification of the molecule by acrolein, a highly reactive component of cigarette smoke [28]. Other studies have shown that cigarette smoke reduces CFTR channel open probability, further reducing mucociliary clearance. Other related mechanisms impairing CFTR channel function include redox-related injury because of acute and chronic inflammation and infection. Reduced CFTR function causes increased ENaC activity and hyperabsorption of Na^{+}, further contributing to airway dehydration [29]. However, data on ENaC activity in COPD is less conclusive than those on CFTR activity [30]. Studies in CFTR knockout mice demonstrated elevated ENaC activity. However, another study on a CF pig model did not show increased transepithelial sodium absorption in the absence of CFTR protein [29]. Tarran et al in 2014 demonstrated that ENaC inhibition increases airway hydration and prevents cigarette smoke induced ASL height depletion [31].

1.8. Therapeutic approaches in diseases with impaired CFTR function

1.8.1. Symptomatic treatment: aiming the improvement of mucus clearance

Improvement of mucus clearance in CF and COPD is key to preventing declines in lung function [32]. Even in CF where CFTR-corrective therapies are available, there is a group of patients (e.g., with nonsense mutations) who will still rely on symptomatic treatment via CFTR-independent approaches. In addition, patients treated with CFTR modulators will still benefit from therapies improving mucus clearance.

1.8.1.1. Osmotic agents

These are compounds that cause water to be drawn into the lumen of airways, to reduce dehydration of the ASL in CF and COPD because of compromised ion transport [29]. Inhalation of hypertonic saline (7% NaCl) is clinically effective although the precise underlying mechanisms are not completely understood. The current hypothesis is that

administration of hypertonic saline causes fluid influx into the airway lumen. Once water flows into the lumen, it swells the ASL. Mucus hyperconcentration in CF provides a further osmotic driving force. Another osmotic agent is mannitol, which has been proved to be effective in improving ASL hydration. It has been approved for clinical use in the EU, Australia, Israel and USA. Mannitol is an inert sugar that is not absorbed, nor metabolized and does not cross the blood-brain barrier. Just like hypertonic saline, mannitol creates an osmotic gradient and draws water into the airway lumen [32].

1.8.1.2. Surfactants

Surfactants are agents that are capable of reducing the surface tension between a liquid and another substance. Application of surfactants can interact with the hydrophobic regions of the mucin network and the interface of ASL. The disruption of hydrophobic interactions disperses the mucin-rich fraction of the gel, creating a single-phase gel and reducing viscosity. Mucin polymers cannot interact with each other in the presence of surfactants, therefore the affinity of the surface is reduced and water solubility is increased. However, clinical data on surfactants is conflicting, some studies show positive results in patients with chronic bronchitis, and some concluded surfactants neither worsen, nor improve the condition of CF patients [32, 33, 34].

1.8.1.3. Reducing agents

A “classical” therapy that has been used for decades in patients with thick airway mucus aims to fragment the mucin network itself, are the mucolytics. The most common and most effective “mucolytic” used in CF is inhaled dornase alfa, a recombinant human DNase that digests the extracellular DNA in mucus, that is released from dying neutrophils in the gel. It is most effective in patients with inflammation but was found to be ineffective in COPD patients [35]. Another widely used drug is N-acetylcysteine (NAC/ACC) which is a thiol-based compound that cleaves intra- and intermolecular disulfide bonds. The concept that reducing mucin disulfide bonds decreases viscoelasticity of mucus has been demonstrated and can be explained by physics. However, this drug shows only limited efficacy in vivo. The explanation might be that

NAC possesses a low intrinsic reducing activity when inhaled, because it mostly remains in its inactive form at physiological pH and the drug is rapidly cleared/absorbed from epithelial surfaces [32].

1.8.1.4. Chelating agents

In CF, the secretion of bicarbonate, an alkalinizing but also a chelating agent, is diminished. As a result, mucin expansion is impaired after secretion to the apical surface. The addition of high concentrations of bicarbonate to CF airway model systems has been shown to change the proportion of condensed/expanded mucins.
Ethylenediaminetetraacetic acid (EDTA) is also capable of chelating metal ions, so it has been used in CF models to bind calcium and normalize mucus properties. In CF mice EDTA induced rheological changes that were similar to bicarbonate at 6-fold lower concentration. A similar compound more selective to calcium, EGTA has also been used in CF research to provide calcium chelation [32]. Unfortunately, tissue integrity has been compromised by both 20 mM EDTA and 115 mM bicarbonate, suggesting these compounds are likely not suitable for human treatment at high concentrations [36].

OligoG, a guluronate-rich alginate with high affinity for Ca^{2+}, facilitated the removal of adherent mouse ileum mucus at low concentrations (1,5 %) while tissue integrity remained intact. It has been hypothesized that this effective concentration can be reached in the lungs via dry powder inhalation. Preliminary data from Phase II clinical trial showed that although there was not a significant difference in mucociliary clearance, a more peripheral deposition of tracer particles was observed in subjects treated with oligoG, suggesting the opening of previously occluded airways [37].

Another chemical agent, a polycationic bipolymer, poly (acetyl, arginyl) glucosamine (PAAG) was used in *in vitro* and *in vivo* models of CF to displace Ca^{2+} and support proper expansion and linearization of mucus after exocytosis. PAAG not only significantly improved the viscoelastic properties of the sputum in CF but it increased ciliary beat frequency. Treatment of CFTR knockout ferrets by aerosolization resolved intestinal and airway plugging, and also lowered the levels of inflammatory markers, suggesting that

Ca^{2+}-chelating agents may be a valid therapeutic approach to treat patients with defective CFTR [32].

1.8.1.5. Non-CFTR ion channel agents

Direct modulation of mucus properties via ion channel targeting [30] could be an effective strategy not only in patients with CF, but also in patients with COPD, especially in those individuals who suffer from chronic bronchitis and/or mucus stasis and accumulation.
ENaC blockers have the potential to improve ASL hydration by inhibiting excessive Na^+ absorption via the ENaC channel. However, ENaC-blocking small molecule therapies turned out to be unsuccessful due to the short half-life of these molecules in the airways and effects on renal Na^+ transport is the key dose limiting safety concern. In CF, the upregulation of ENaC is partly due to the degradation of SPLUNC1 (an inhibitory protein that promotes ENaC internalization) by neutrophil elastase which can be found in high concentration in CF sputum. SPX-101, an ENaC blocker (Spyryx Biosciences) is a peptidomimetic compound that resembles the ENaC -inhibiting region of the SPLUNC1 protein and is not a substrate of proteases in CF sputum [38]. Phase II study showed a 5,2% increase in FEV_1 in SPX-101 treated patients compared to the placebo control group. Another therapeutic approach is to potentiate other chloride channels expressed in airway epithelium. TMEM16A or anoctamin-1 is a voltage-sensitive calcium-activated chloride channel expressed in epithelial cells. TMEM16A potentiators are being tested *in vitro* and the drugs were reported to positively stimulate anion conductance and fluid secretion in CF cell cultures [39, 32].

Raising intracellular calcium level potentiates the alternative chloride secretion pathway. Purinergic receptors were first described in 1976, 2 years later two types of purinergic receptors were distinguished: P1 and P2 receptors [40]. P1 receptors are activated by adenosine and coupled by G-proteins, often referred to as adenosine receptors (ADOR). There are four subtypes of P1 receptors: ADORA1 and ADORA3 inhibits adenylate cyclase and lower cAMP levels, ADORA2A and ADORA2B activates adenylate cyclase, increasing cAMP levels. ADORA2B also activates phospholipase C and increases intracellular calcium levels. The other large group of purinergic receptors are the P2 receptors, which recognize primarily extracellular ATP, ADP, UTP and UDP [41]. One

subtype of this nucleotide-receptor family is the P2Y receptors. These are metabotropic, G-coupled receptors, releasing Ca^{2+} from intracellular stores. There are eight subtypes: P2Y1, P2Y2, P2Y4, P2Y6, P2Y11, P2Y12, P2Y13 and P2Y14 (the missing numbers are non-mammalian orthologs or receptors unresponsive to nucleotides). These subtypes can be activated by a variety of nucleotides with different potencies [41]. However, denufosol, a P2Y2-receptor agonist that stimulates intracellular calcium elevation and activates Ca-dependent chloride channels made its way to clinical trial (2008), but it failed to improve pulmonary functions in CF patients [32]. This ineffectiveness might be due to the rapid agonist-induced desensitization and sequestration of the P2YRs [42].

Another subclass of P2 nucleotide receptors is the P2X receptor channels (P2XR). These receptors function as ATP-gated nonselective cation channels. They are permeable to both mono- and divalent cations such as sodium and calcium, respectively. These receptors are sensitive to the extracellular ion milieu. However, their sensitivity to pH and other ions (such as divalent cations) differ in receptor subtypes. P2X2 receptors are potentiated by H^+ while, for example P2X1Rs, P2X4Rs are inhibited by acidification [43]. Moreover, extracellular H^+ appears to have a dual effect on P2X3Rs: acidification of the extracellular milieu inhibits ion currents at low agonist concentration (probably due to decrease in activation), and increases ion currents at high agonist concentration (probably due to slower desensitization) [44]. Ma et al demonstrated that extracellular Na^+ regulates airway ciliary motility by inhibiting P2XRs, therefore, lowering external Na^+ enhances ciliary beat and P2X channel activity [45]. The same research group concluded that extracellular Na^+ concentration may play a fundamental role in P2X regulation as Na^+ both inhibits and permeates P2XRs [46]. These receptors are also sensitive for extracellular H^+ concentration: alkaline extracellular pH further induced Ca^{2+} entry via P2XRs, while acidic extracellular pH inhibited Ca^{2+} influx [47]. Also, P2XRs are also modulated by divalent cations such as Zn^{2+}, Cu^{2+}, Mg^{2+} and Ca^{2+} [48, 49]. These ions can either potentiate or inhibit P2XRs depending on the composition of different receptor subtypes expressed on the cells. P2XRs has seven subtypes (P2X1-7) with a topology of intracellular termini and two transmembrane domains (TM), with TM1 involved in channel gating, and TM2 lining the channel pore [41]. The large extracellular loop contains regions of acidic residues to attract cations. The functional ion channel is formed from three subunits and can be homo- or heterotrimeric, with three binding sites for ATP. Previously it was believed that all binding sites must be occupied for the channel pore to open. More recent studies confirmed that occupation of two binding sites out of three is

enough to open the channel pore [50]. P2X1 and P2X3 have high affinity for ATP and activate and desensitize rapidly. P2X2 and P2X4 have lower affinity for ATP, with sustained currents and slow desensitization after activation. P2X7 has a very low ATP potency with little desensitization, while P2X5 and P2X6 might require heteromerization to function, because alone they appear to be non-functioning [51]. Expression of P2X4 and P2X6 receptor isoforms in bronchial epithelium has been shown by in situ hybridization [52, 53]. There is evidence that P2X4 receptors on human airway epithelial cells (16HBE14o-) mediated ATP-induced Ca^{2+} entry that caused a sustained intracellular Ca^{2+} increase [47]. In an alkaline, sodium-free environment Zn^{2+} acts as a full agonist of P2XRs in human control and CF airway epithelial cell lines [54]. Small interference RNA fragments specific to P2X4 and P2X6 (but not P2X5) significantly inhibited Zn^{2+}-induced Ca^{2+} entry on IB3-1 (CF human airway epithelial cell line) cells, suggesting that multiple P2X receptor subtypes are involved [55]. Besides modulation of P2XR function, zinc can bind to zinc-sensing receptors (ZnRs), that are $G_{\alpha q}$-coupled and release Ca^{2+} from intracellular stores [56]. Zinc is also proved to inhibit store-operated calcium channels (SOCs), acting as a competitive inhibitor of Ca^{2+} influx but does not permeate through the channel [57]. Gore et al identified a high-affinity binding site on SOCs for zinc [58]. Therefore, the ATP induced calcium signal can be further potentiated or inhibited by zinc, extracellular sodium concentration and pH (Figure 3.).

DOI:10.14753/SE.2024.3008

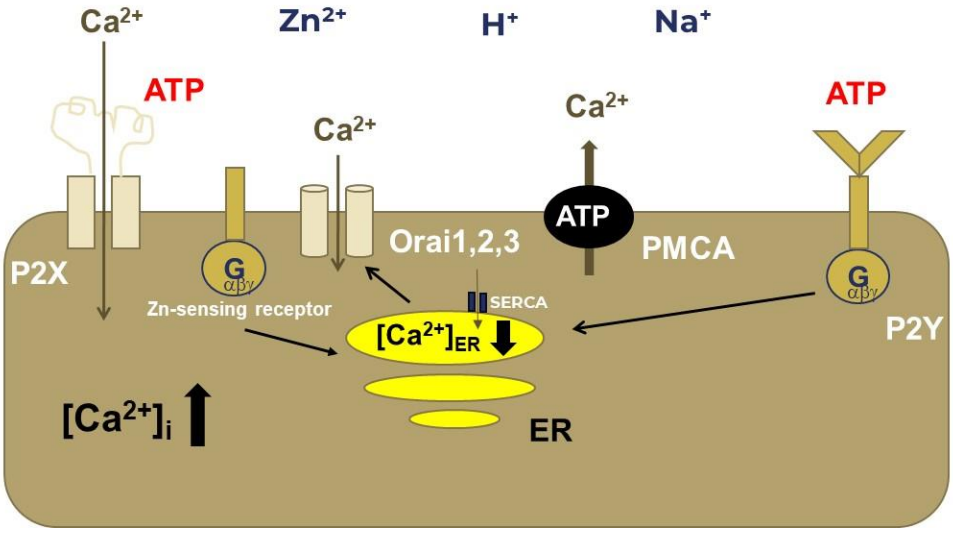

Figure 3. Activation of purinergic receptors and regulation of calcium homeostasis. ATP binds to G-protein coupled P2Y receptors, and Ca^{2+} is released from the stores of endoplasmic reticulum (ER). P2X receptors are receptor channels, and their activation increases intracellular Ca^{2+} via Ca^{2+} influx from the extracellular space. Emptying the Ca^{2+} stores of ER activates store operated Ca^{2+} channels (namely Orai1, 2 and 3) and intracellular stores are re-loaded through SERCA (sarcoplasmic/endoplasmic reticulum Ca^{2+}-ATPase). Elevation of intracellular Ca^{2+} concentration $[Ca^{2+}]_i$ activates PMCA (plasma membrane Ca^{2+}-ATPase) and Ca^{2+} is transported to the extracellular space. Besides modulation of receptors on the cell surface (such as P2XRs and SOCs) Zn^{2+} also binds to a G-protein coupled zinc-sensing receptor. Changes in pH and sodium concentration in the extracellular milieu further potentiate or inhibit ATP-induced Ca^{2+} signals.

1.8.2. Curative treatments to improve CFTR function

Symptomatic treatments for CF and COPD are detailed above, however there are some specific drugs, aiming directly at the improvement of CFTR function as a gene-based therapy in CF treatment. These treatment strategies are specific to the CFTR mutation and aim to bypass specific preterm termination codons and restore mRNA levels (for Class I mutations), or correct CFTR trafficking to the apical plasma membrane (for Class II mutations) or increase the CFTR channel function [59]. The first agent for the latter was ivacaftor [60], which was approved by the Food and Drug Administration (FDA) to be used in patients older than 6 years of age with at least one1 G551D mutation in the CFTR gene. This is a Class III defect, when the CFTR protein reaches the cell membrane

but its channel opening function is impaired. Ivacaftor allows the opening probability of the channel to be increased, so it is classified as a CFTR potentiator. In 2015 ivacaftor was approved to be combined with a corrector lumacaftor for homozygous ΔF508 CF patients. Most recently, the addition of a second site CFTR corrector agent to a potentiator-corrector combination was shown to improve lung function in both hetero- and homozygous ΔF508 CF patients, leading to the registration of the ivacaftor-tezacaftor-elexacaftor (Trikafta) fixed dose combination in the US in 2019 [61]. Other therapies in preclinical development are not mutation specific and include gene therapy to edit the genome and stem cell therapy to repair airway tissue [59]. Amplifiers are drugs to treat mutations leading to decreased CFTR synthesis (Class IV) by stimulation of protein expression. The PTI-428 compound from Proteostasis Therapeutics is a first-in-class CFTR amplifier that showed an *in vitro* increase in CFTR protein levels. It is able to improve mRNA stability and/or assist the process surrounding CFTR transcription and translation [59]. Another group of therapy strategies are the so-called stabilizers, which can rectify the intrinsic protein instability and increase the time that mutant CFTR remains in the plasma membrane and decrease the protein degradation rate from the membrane. Cavosonstat (an inhibitor of S-nitrosogluthatione reductase) increases S-nitrosogluthatione levels and leads to CFTR maturation and plasma membrane stability. A phase II clinical study is being conducted to test Cavosonstat for patients with two copies of ΔF508 mutations in combination with CFTR potentiators.

1.8.3. Treatments for COPD

Current pharmacological treatments offer no significant benefits concerning disease outcome. However, the major modifiable risk factor is smoking, other treatments are also necessary to slow the progression of worsening respiratory functions. Bronchodilators frequently combined with inhaled corticosteroids remain to be the core of the treatment to reduce acute exacerbations, improve respiratory functions and life quality, however they do not improve mortality associated with COPD. Inhaled steroids enhance the risk of pneumonia and have no effect on mucus clearance [21].

DOI:10.14753/SE.2024.3008

2. Objectives

2.1. One of the therapeutic approaches for defective CFTR function is activation of alternative anion channels, such as the Ca-activated chloride channel in the airway epithelium. The calcium homeostasis of epithelial cells is regulated by calcium influx from extracellular space, calcium release by intracellular stores and calcium elimination. Our aim was to test the effect of extracellular pH, ATP and divalent cations (including zinc) on the intracellular calcium level of airway epithelial cells to determine the ideal composition of aerosols in which a drug can be applied to improve mucociliary clearance and ASL hydration in diseases with CFTR dysfunction.

2.2. Despite the different pathogenesis, CF and COPD share common pathological features, such as compromised CFTR function, impaired mucus clearance and airway acidification. The latter could be due to defective bicarbonate transport through the CFTR anion channel. Therefore, we hypothesized that bicarbonate-containing aerosols could be beneficial for patients with CFTR dysfunctions. Our aim was to test the safety and efficacy of chronic bicarbonate inhalation in a COPD animal model, as a model for impaired CFTR function.

DOI:10.14753/SE.2024.3008

3.Methods

3.1. Effect of extracellular pH, ATP and divalent cations on the intracellular Ca^{2+} level of airway epithelial cells

3.1.1. Materials

ATP, Thapsigargin, U-73122, BZ-ATP, suramin, hexokinase and apyrase were purchased from Sigma Chemical (St. Louis, MO). Fluo- 3/AM was purchased from Invitrogen Inc. (Carlsbad, CA). All other chemicals were purchased from Reanal Inc. (Budapest, Hungary).

3.1.2. Culturing and maintenance of CFTR-transfected CFBE41o− cells

The human airway epithelial cell line (CFBE41o−) was a generous gift from Dr. Erik M. Schwiebert and Dr. Zsuzsa Bebők (University of Alabama at Birmingham, Birmingham, AL). The CFTR expressing CFBE41o− cells were stably transfected with either wild-type or delF508 CFTR cDNA and selected by puromycin resistance. Details of the transfections are described by Bebok et al. [62]. Cells were grown in plastic tissue culture flasks in Dulbecco's modified Eagle's/Ham-F12 (1:1) medium supplemented with 10% fetal bovine serum and 100 g/ml penicillin/streptomycin. Two days before the experiments cells were plated and grown on a round glass coverslip at 37℃.

3.1.3. Recording solutions

At the beginning of each experiment, we superfused the cells with a standard solution (Na–Ca–7.4-sol) containing NaCl 145 mM, KCl 5 mM, $CaCl_2$ 3 mM, $MgCl_2$ 1 mM, HEPES 10 mM, glucose 10 mM, (pH 7.4). Sodium was substituted with either equimolar N-methyl-d-glucamine (NMDG–Ca–7.4-sol) or lithium (Li–Ca–7.4-sol). The Ca^{2+} depleted solutions were prepared by omitting $CaCl_2$ (Na–7.4-sol or NMDG–7.4-sol). The effects of alkaline external conditions were tested at pH 7.9. In some experiments, to empty intracellular Ca^{2+} stores 0.1 M thapsigargin was used for 15 min prior to the recording. Experiments were performed at room temperature under a continuous flow of solutions with a speed of 3 ml/min. The volume of the chamber was 1.5 ml therefore complete change of the bath solution took approximately 30 s.

3.1.4. Measurement of intracellular calcium

CFBE41o− cells were loaded with Fluo-3/AM (4 μM) in the Na–Ca–7.4-sol for 60 min at room temperature. The cells were then washed with Na–Ca–7.4-sol, and the coverslips were mounted into a perfusion chamber equipped with an inverted microscope. Recordings were made with a confocal laser scanning microscope, Axiovert 200M Zeiss LSM 510 Meta (Carl Zeiss, Jena, Germany) equipped with a 20× Plan Apochromat (NA = 0.80) DIC objective which is able to acquire data in real-time enabling Ca^{2+} dynamics of individual cells in vitro. We used a 488-nm argon-ion laser for the excitation. The emitted light was collected with BP 505–570 band pass filter. A few cells apparently demonstrated high or low basal levels of cytosolic Ca^{2+} that we excluded from our experiments. Studies were conducted preferentially with clones emitting medium fluorescence as judged by the eye. This was done by selecting regions of interest (ROIs). Each measurement was stored in the form of digital video recording. The average fluorescence of the chosen area was obtained at a rate of 0.5 Hz.

3.1.5. Data presentation

Changes in intracellular calcium concentration ($[Ca^{2+}]_i$) are displayed as the percentage of fluorescence relative to the intensity at the beginning of each experiment. Baseline fluorescence (100%) was calculated from the average fluorescence at the ROIs during perfusion of the cells with Na–Ca–7.4-solution. The autofluorescence was subtracted from the readings by measuring a cell-free area on the same coverslip. The velocity of changes in $[Ca^{2+}]_i$ was estimated by the slope of the curves (% / min). In some experiments when two substances were administered in a consecutive manner a ratio of fluorescence intensity % was calculated from the data obtained 5 min after and immediately prior to administration of the second substance. Therefore, an increase or decrease of the ratio indicated additional Ca^{2+} entry or accelerated decline of the Ca^{2+} signal, respectively. The average results are expressed as mean ± standard error of the mean (S.E.M.) and each n represents the mean of a single coverslip containing at least 20 cells. Statistical comparisons were made using F-probe and Student's paired t-test. Differences were considered statistically significant when $p < 0.05$.

3.1.6. Measurements of inositol-trisphosphate (IP_3) buffering

For single cell Ca^{2+} measurement cells were plated onto 25-mm diameter circular glass coverslips at a density of 3 × 105 cells / 35-mm wells on day before transfection with plasmid DNA of the mRFP-IP3 R-LBD constructs [63] (1 g / dish) using the Lipofectamine 2000 reagent (Invitrogen) and OPTI-MEM (Invitrogen). On day after transfection cells were loaded with Fura-2/AM (2 μM, 45 min) at room temperature in a modified Krebs–Ringer buffer containing 120 mM NaCl, 4.7 mM KCl, 1.2 mM $CaCl_2$, 0.7 mM $MgSO_4$, 10 mM glucose, Na-Hepes 10 mM, pH 7.4 in the presence of 200 M sulfinpyrazone and 0.04 % pluronic acid. Ca^{2+} measurements were performed at room temperature in NMDG solution containing no Ca^{2+}. An inverted microscope (Axio Observer, Zeiss) equipped with a 40× oil immersion objective (Fluar, Zeiss) and a Cascade II camera (Photometrics) was used. Excitation wave- lengths were set by a random access monochromator connected to a xenon arc lamp (DeltaRAM, Photon Technology International). To identify cells expressing mRFP-IP3R-LBD, mRFP fluorescence was measured at the beginning of each experiment using an excitation wavelength of 570 nm with a 610 nm dichroic filter and a 640 nm filter set. For ratiometric measurements of Fura-2 excitation wave- lengths of 340 and 380 nm were selected combined with a 505 nm dichroic filter and a 525/536 nm emission filter set. Data acquisition and processing were performed by the MetaFluor (Molecular Devices) software. Images were acquired every 5 s for a period of 5 min. For time resolved measurement of fluorescence, 340/380 nm ratio value was calculated from the background subtracted recordings.

3.1.7. Immunohistochemistry

For the immunofluorescent staining, the CFBE41o− cells were seeded and cultured on 12 mm diameter coverslips in plastic culture wells. At 70 % confluence, the culture was placed into a wet chamber and washed in PBS and then fixed in acetone for 5 min. After washing in PBS we used 1 % BSA for 30 min to block nonspecific labeling. The primary antibodies used were goat polyclonal anti-P2X4, anti-P2X5 and anti-P2X6 (Santa Cruz Biotechnology Inc.) and were incubated overnight at +4 °C. (dilution: 1:100 in BSA). For the double labeling we used rabbit polyclonal anti-P2X4, anti-P2X5 and anti-P2X6 (Alomone Laboratories Ltd.) together with the above-mentioned antibodies. After washing in PBS, we used FITC conjugated rabbit anti-goat secondary antibody (Vector

Laboratories Inc.) (dilution: 1:200 in PBS). The incubation time was 45 min at room temperature in the dark. For the double labeling, the secondary antibodies were FITC conjugated donkey anti-goat antibody and TexasRed conjugated bovine anti-rabbit antibody. (Vector Laboratories Inc.) (dilution: 1:100). After washing, we used a mounting media containing DAPI or Propidium iodine for the nuclear staining. (Vector Laboratories Inc.). The samples were then visualized, and pictures were taken with the Zeiss laser scanning microscope. The same setting parameters were used.

3.2. Effect of HCO_3^- inhalation in COPD animal model

3.2.1. Animals

Experiments were performed on 8-week-old male guinea pigs weighing 600±150 g at the beginning of the study. Animals were bred and kept in the Laboratory Animal House of the Department of Pharmacology and Pharmacotherapy, University of Pécs, Hungary at 24–25 °C, provided with standard chow, vegetables and fruits and water ad libitum, maintained under 12 h light–dark cycle. All procedures were performed in accordance with the 40/2013 (II.14.) Government Regulation on Animal Protection and Consideration Decree of Scientific Procedures of Animal Experiments and Directive 2010/63/ EU of the European Parliament. They were approved by the Animal Welfare Committee of the University of Pécs and the National Scientific Ethics Committee on Animal Research of Hungary (licence No.: BA02/2000–4/2019 issued on 29 Jan 2019 by the Government Office of Baranya County).

3.2.2. Experimental design

Guinea pigs were divided into 4 groups (4 animals / group); 2 groups treated with hypertonic NaCl (8.4 % corresponding to 1.44 M) and the other 2 groups with hypertonic $NaHCO_3$ (8.4 % corresponding to 1 M) aerosol for 30 min, twice daily, 5 days/week, for 8 weeks. Hypertonic NaCl and $NaHCO_3$ solutions were prepared freshly each week and were aerosolized by a nebulizer (1–5 μM particle size**;** Boneco 7145 W ultrasonic nebulizer, BonAir BG Ltd., Budapest, Hungary) into 55×35×40 cm boxes where guinea pigs were placed during inhalation treatment. The treatment groups were subdivided into groups inhaling only NaCl or $NaHCO_3$, and groups exposed to cigarette smoke besides the respective aerosol treatments. Cigarette smoke exposure (CSE) was performed after

aerosol treatment in a whole-body smoke exposure chamber (Teague Enterprise, USA) for 30 min followed by a ventilation period of 30 min twice daily, 10 times/ week for 8 weeks with the use of 2 research cigarettes at a time (3R4F Kentucky Research Cigarette; University of Kentucky, USA) [64]. Body weight was measured daily, respiratory functions were assessed at the beginning and at the end of week 2, 4, 6 and 8. At the end of the experimental protocol animals were anesthetized by pentobarbital sodium (1 % Euthanimal 400 mg/ml, Alfasan, the Netherlands; 0.5 ml/100 g) and arterial as well as venous blood was collected for laboratory tests. Lungs were excised and fixed in 6 % formaldehyde solution for histopathological assessment.

3.2.3. Investigation of respiratory functions

Airway function was measured by unrestrained whole-body plethysmography (PLY3213 Buxco Europe Ltd., Winchester, UK) at the beginning and at the end of week 2, 4, 6 and 8 in conscious, spontaneously breathing guinea pigs. Breathing frequency, tidal volume, minute ventilation, inspiratory and expiratory times, peak inspiratory and expiratory flows, as well as baseline enhanced pause correlating with airway resistance were measured for 15 min following a 15-min-long acclimation period.

3.2.4. Histopathological evaluation

Lung samples were fixed in 6 % paraformaldehyde solution and embedded in paraffin. Hematoxylin–eosin staining was performed on 5 μm sections for the assessment of lung pathophysiology. Three different localizations (apex, hilus, base) were excised from the lungs of each animal. Slides were examined using a brightfield microscope (Olympus CH30). Ten non-cartilaginous airways, ten vessels and ten septa (examined by high power field) were selected from each lung site of every group (equally chosen from each animal). Acute inflammatory cell infiltration (eosinophil and neutrophil granulocytes) was counted in the airways, vessels and septa to evaluate the extent of airway inflammation [**65**]. Airway intraluminal perimeter was measured with Case Viewer software (3DHISTECH Ltd, Hungary) after scanning each slide with 20× objective (Pannoramic 250 FLASH III scanner, 3DHistech Ltd., Hungary). Airway intraluminal perimeter was used to normalize airway dimensions.

3.2.5. Laboratory parameters

Urine pH was assessed every week of the experimental protocol. Animals were placed in a metabolic cage for the period of urine collection. pH was assessed from freshly collected urine by a FiveEasyPlusTM pH meter (Mettler Toledo, Hungary). At the end of the experimental protocol arterial blood was collected for blood gas and acid base analysis by Astrup's equilibration technique in the Department of Laboratory Medicine, University of Pécs, Hungary. Other laboratory parameters were measured from heparinized venous blood by an AU5800 clinical chemistry analyzer (Beckman Coulter Hungary, Budapest, Hungary) in the Department of Laboratory Medicine, Semmelweis University, Budapest, Hungary.

3.2.6. Statistical analysis

Statistical analysis was performed by GraphPad Prism v6 software (GraphPad, San Diego, CA, USA). Respiratory parameters and body weight were analyzed by repeated measures two-way ANOVA followed by Tukey's multiple comparisons test. Histopathological and laboratory parameters were assessed by Kruskal–Wallis followed by Dunn's multiple comparisons test.

DOI:10.14753/SE.2024.3008

4. Results

4.1. Regulation of P2X-mediated calcium entry by extracellular ionic environment

4.1.1. Purinergic receptor stimulation elicits similar Ca^{2+} signals in wild-type-CFTR and F508del-CFTR expressing cells (CFBE41o-)

In order to test the effects of ATP on Ca^{2+} signal in CFBE41o− cells transfected either with ΔF-CFTR or wt-CFTR. In both ΔF-CFTR and wt-CFTR cells, ATP (100 μM) provoked a biphasic increase in $[Ca^{2+}]_i$. An initial Ca^{2+} peak was followed by a sustained increase of $[Ca^{2+}]_i$. Moreover, ATP elicited a monophasic response in Ca^{2+}-depleted extracellular saline suggesting that Ca^{2+} entry from the extracellular space was necessary for the sustained phase of Ca^{2+} signal (Figure 4.). It has been shown that in airway epithelial cells, Ca^{2+} influx through the plasma membrane is modified by the external pH and Na^+ concentration [47, 54]. We raised the pH of the bath solution from 7.4 to 7.9 prior to the administration of ATP (100 μM), to test whether extracellular alkalinization would stimulate Ca^{2+} entry. Under these conditions we observed neither in ΔF-CFTR nor in wt-CFTR cells potentiation of the ATP-induced Ca^{2+} signal (data not shown). When external pH was elevated (7.9) with parallel substitution of extracellular Na^+ by a non-permeant large organic cation NMDG, ATP (100 μM) elicited a significantly higher sustained Ca^{2+} signal in both ΔF-CFTR and wt-CFTR cells. These data suggested that changes in the external ionic environment modify ATP-induced Ca^{2+} signals independent of the CFTR mutations (Table 1.).

DOI:10.14753/SE.2024.3008

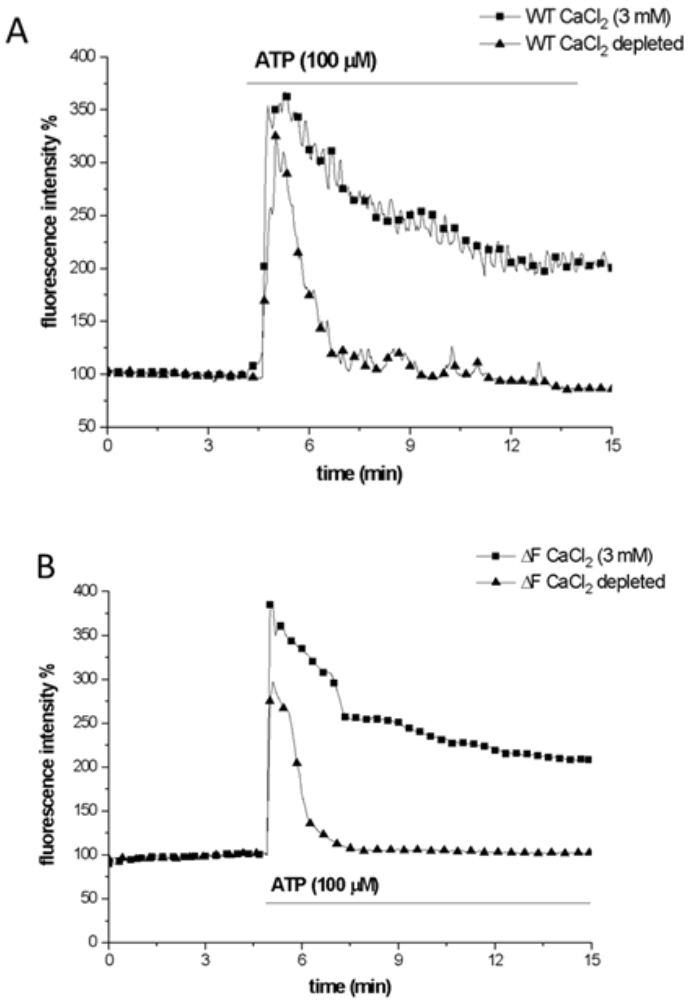

Figure 4. Effects of ATP on $[Ca^{2+}]_i$ in CFBE cells. (A) Original traces showing the effect of ATP (100 μM) on $[Ca^{2+}]_i$ of WT cells perfused with Na^+-containing solution at pH 7.4 in presence of $CaCl_2$ (3 mM) and following extracellular Ca^{2+} depletion. (B) Effect of ATP (100 μM) on $[Ca^{2+}]_i$ in ΔF cells perfused with Na^+-containing medium at pH 7.4 in the presence of $CaCl_2$ (3 mM) and following extracellular Ca^{2+} depletion. The average of fluorescence intensity between the second and the third minute of each experiment was considered as 100%. Each experiment was performed 10 times using cells from at least two different passages with similar results.

Based on figure from Hargitai D, Pataki A, Raffai G, Füzi M, Dankó T, Csernoch L, Várnai P, Szigeti GP, Zsembery A. Calcium entry is regulated by Zn^{2+} in relation to extracellular ionic environment in human airway epithelial cells. Respir. Physiol. Neurobiol. 2010 Jan 31;170(1):67-75.

Table 1. Effects of ATP (100 μM) on WT and ΔF cells at pH 7.4 and pH 7.9 in the presence and the absence of Na^+ (replaced with $NMDG^+$). Two components of Ca^{2+} signal were assessed: peak increase of fluorescence intensity after administration of ATP (ATP_{max}) and the intensity detected at the beginning of ATP washout (ATP_{end}). # vs. WT ATP_{end} pH 7.4 ($p < 0.001$). § vs. WT ATP_{max} pH 7.4 ($p < 0.01$). §§ vs. WT ATP_{max} pH 7.9 ($p < 0.001$). §§§ vs. WT ATP_{max} Na^+-free, pH 7.9 ($p < 0.05$). * vs. ΔF ATP_{end} pH 7.4 ($p < 0.001$). Mean: average of fluorescence intensity %, fluorescence intensity of baseline was considered as 100%, recorded between 2. and 3. minute of Na-Ca-7.4-solution administration. SE: standard error, N: number of cells detected. Cells were obtained from at least two different passages.

Based on table from Hargitai D, Pataki A, Raffai G, Füzi M, Dankó T, Csernoch L, Várnai P, Szigeti GP, Zsembery A. Calcium entry is regulated by Zn^{2+} in relation to extracellular ionic environment in human airway epithelial cells. Respir. Physiol. Neurobiol. 2010 Jan 31;170(1):67-75.

	WT					ΔF508				
	ATP_{max}		ATP_{end}			ATP_{max}		ATP_{end}		
	Mean	SE	Mean	SE	N	Mean	SE	Mean	SE	N
EC pH 7.4	343.86	7.8	224.38	7.5	160	379.60 §	10.4	215.23	7.3	160
EC pH 7.9	314.17	9.1	198.41	6.9	160	400.93 §§	10.1	201.56	6.0	117
NMDG pH 7.9	365.85	9.6	279.19 #	8.7	160	392.57 §§§	8.7	283.20 *	5.8	160

4.1.2. Effects of Zn^{2+} on ATP-induced Ca^{2+} signal in airway epithelial cells expressing wild-type or F508del-CFTR

There is evidence that Zn^{2+} interacts with many Ca^{2+} channels, such as P2XRs and SOCs. Metal ions mainly inhibit SOCs [66], while Zn^{2+} either potentiates or inhibits P2XR receptors depending on the composition of different subtypes expressed on the cells [49]. Besides, Zn^{2+} can also bind to divalent cation-sensing receptors, that are $G_{\alpha q}$-coupled and release Ca^{2+} from intracellular stores in different epithelial cells [56, 67, 68, 69]. Therefore, we have speculated that Zn^{2+} could influence ATP-induced Ca^{2+} signal in CFBE41o− cells by either interacting with Ca^{2+} entry channels or by stimulating G protein-coupled divalent cation-sensing receptors. To our surprise in NaCl-rich (145 mM) external solution, $ZnCl_2$ (20 μM) inhibited the ATP-induced sustained Ca^{2+} plateau both

in wt-CFTR and ΔF-CFTR expressing cells while peak increase of $[Ca^{2+}]_i$ induced by ATP was not influenced by Zn^{2+}. Increasing the pH from 7.4 to 7.9 suspended inhibitory effects of Zn^{2+} on ATP-elicited sustained Ca^{2+} signal (Figure 5.). This so called Ca^{2+} plateau is a result of a new balance between Ca^{2+} extrusion and Ca^{2+} influx, suggesting that Zn^{2+} either inhibits P2XRs or SOCs (activated due to ATP induced intracellular Ca^{2+} store depletion). We hypothesized that in NaCl rich extracellular solution Zn^{2+} rather inhibits SOCs than P2XR, as previous results indicated that Zn^{2+} is able to inhibit SOCs [54]. Moreover, in human erythrocytes Zn^{2+} interacted with plasma membrane Ca^{2+} ATPase (PMCA) [70]. Taken together, two possibilites emerged: Zn^{2+} either inhibited SOC-mediated Ca^{2+} entry or stimulated PMCA activity. To exclude interaction with PMCA, we have pretreated the wt-CFTR expressing cells with thapsigargin that is known to activate SOCs by emptying intracellular Ca^{2+} stores. In Ca^{2+}-depleted extracellular saline, administration of $BaCl_2$ (3 mM) caused an increase in fluorescence due to Ba^{2+} entry which was arrested by Zn^{2+} ($slope_{Ba^{2+}} = 26.7 \pm 6.2\%$ / min, n = 3 vs. $slope_{Ba^{2+} + Zn^{2+}} = 8.1 \pm 3.3$ % / min, n = 4, $p < 0.05$). Pretreatment and co-administration of $ZnCl_2$ (20 μM) further slowed down Ba^{2+} entry (4.6 ± 0.8 % / min, n = 4) while removal of Zn^{2+} regained Ba^{2+} influx. Since Ba^{2+} is not a substrate of PMCA [71], these data suggest that zinc inhibits SOCs rather than influences PMCA activity in CFBE41o− cells. Since P2XRs are sensitive to extracellular H^+ concentration, the effects of ATP and Zn^{2+} together were tested at different extracellular pH [72]. Also, it had been shown that extracellular Na^+ directly inhibited P2XRs [45, 46] and might also compete with Ca^{2+} in the passage through these channels [47]. Therefore, we investigated the effects of Zn^{2+} on ATP-induced Ca^{2+} signal following replacement of extracellular Na^+ with a non-permeable cation, NMDG. In sodium-free, NMDG-containing solution, Zn^{2+} significantly increased the ATP-induced Ca^{2+} plateau at both pH 7.4 and 7.9 but did not at pH 6.9 (data not shown). The complete replacement of sodium is a non-physiological condition; therefore, we tested the effects of Zn^{2+} and ATP together at different extracellular Na^+ levels. Our data showed that zinc increased ATP-induced Ca^{2+} signal but only when the Na^+ concentration was 40 mM or less (Figure 6.).

DOI:10.14753/SE.2024.3008

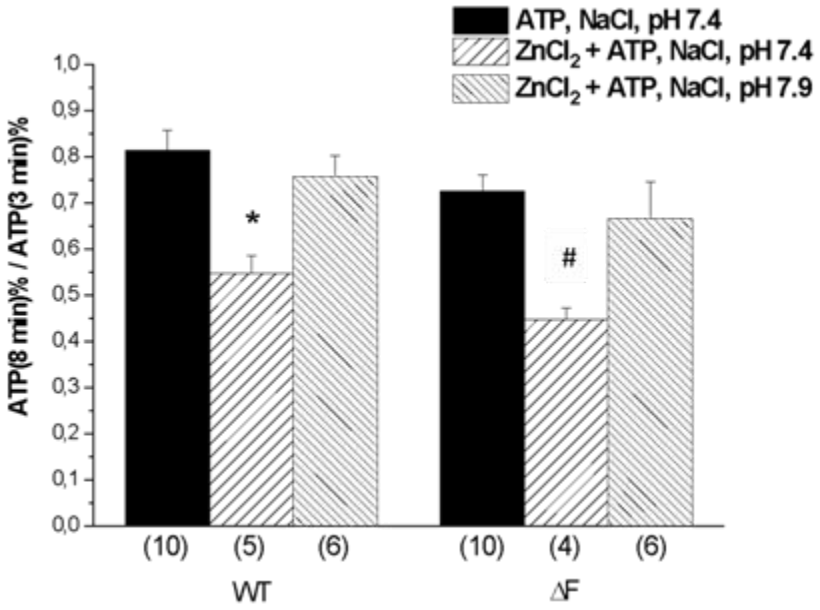

Figure 5. Zn^{2+} accelerates the decay of ATP-induced Ca^{2+} signal in WT and ΔF cells in NaCl-rich environment. Data are expressed as ratio of fluorescence intensity % calculated from data obtained 8 and 3 min after administration of ATP in the presence and absence of Zn^{2+}. $ZnCl_2$ (20 μM) was added after the cells were being perfused with ATP-containing (100 μM) solution for 3 min. * vs. WT ATP, pH 7.4 ($p < 0.001$), # vs. ΔF ATP, pH 7.4 ($p < 0.001$). Data are presented as mean ± S.E.M. The number of independent coverslips is indicated in parenthesis beneath the columns. Each coverslip contained at least 20 cells.

Based on figure from Hargitai D, Pataki A, Raffai G, Füzi M, Dankó T, Csernoch L, Várnai P, Szigeti GP, Zsembery A. Calcium entry is regulated by Zn^{2+} in relation to extracellular ionic environment in human airway epithelial cells. Respir. Physiol. Neurobiol. 2010 Jan 31;170(1):67-75.

DOI:10.14753/SE.2024.3008

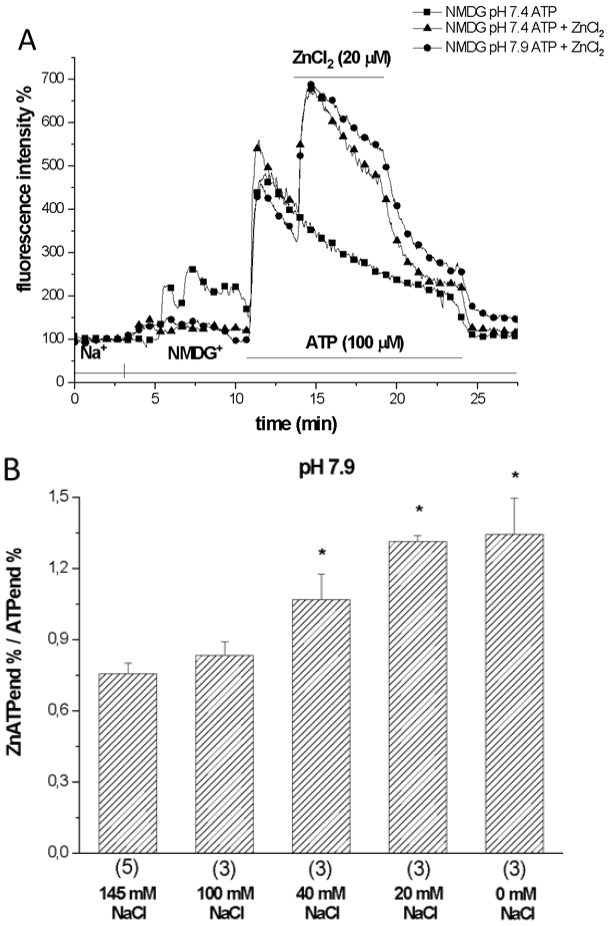

Figure 6. Effect of Zn^{2+} on ATP-induced Ca^{2+} signal in Na^+ -free external solution. (A) Na^+ was replaced with $NMDG^+$. Original traces represent the effect of ATP (100 μM) followed by administration of $ZnCl_2$ (20 μM) at pH 7.4 and 7.9. These experiments were performed 4–6 times using cells from at least two different passages with similar results. (B) Summarized data showing how Zn^{2+} influences the ATP-induced Ca^{2+} -signal at different extracellular Na^+ levels at pH 7.9. The effect of Zn^{2+} was assessed by a ratio of the fluorescence intensity % calculated from data obtained at the end of ATP administration alone and at the end of co-application of ATP and Zn^{2+}. * vs. 145 mM NaCl ($p < 0.05$) The number of independent experiments is indicated in parenthesis beneath the columns.

Based on figure from Hargitai D, Pataki A, Raffai G, Füzi M, Dankó T, Csernoch L, Várnai P, Szigeti GP, Zsembery A. Calcium entry is regulated by Zn^{2+} in relation to extracellular ionic environment in human airway epithelial cells. Respir. Physiol. Neurobiol. 2010 Jan 31;170(1):67-75.

DOI:10.14753/SE.2024.3008

4.1.3. Effects of Zn^{2+} and other divalent metal cations on $[Ca^{2+}]_i$ in CFBE41o− cells expressing wt-CFTR

Our group previously showed that Zn^{2+} induced Ca^{2+} signal (without addition of ATP) in a Na^+ free, alkaline extracellular solution in IB3-1 cells. Therefore, we tested the effects of $ZnCl_2$ (20 μM) without co-administration of ATP. Since Zn^{2+} elicited similar changes in ATP-induced Ca^{2+} signal in both wt-CFTR and ΔF-CFTR expressing cells, these experiments were performed in wt-CFTR expressing cells only. In Na^+-containing solution Zn^{2+} did not change $[Ca^{2+}]_i$. On the other hand, in NMDG-containing solution, Zn^{2+} elicited a sustained increase in $[Ca^{2+}]_i$. The zinc-induced Ca^{2+} plateau was prevented by removal of Ca^{2+} from the external solution whereas the peak of Ca^{2+} signal was reduced by U73122 (10 μM) which is an inhibitor of phospholipase C (PLC). However, U73122 had statistically significant but small effects, we used another approach to confirm the involvement of this pathway in Zn^{2+}-induced Ca^{2+} release from internal stores. The N-terminal IP_3 binding region of the type-I IP_3R was fused to the mRFP for expression in CFBE41o− cells. In Ca^{2+}-depleted solution, Zn^{2+} evoked Ca^{2+} response was significantly reduced in cells expressing this domain if compared with the non-expressing control cells. These data indicate the involvement of the PLC and IP_3 pathway in this process (Figure 7.). To demonstrate whether PLC-dependent Ca^{2+} release could be elicited by other heavy metal divalent cations, we investigated the effects of Ni^{2+} and Cu^{2+}. Administration of $NiCl_2$ (20 μM) caused no change in $[Ca^{2+}]_i$ in NaCl-rich external solution. On the other hand, $CuCl_2$ (20 μM) resulted in a slow and constant increase of $[Ca^{2+}]_i$, suggesting that under these conditions Cu^{2+} induced an irreversible cell damage. When external Na^+ was replaced with $NMDG^+$, both Ni^{2+} and Cu^{2+} induced a sustained and reversible Ca^{2+} signal. Both cations caused a transient Ca^{2+} signal following the removal of extracellular Ca^{2+}, suggesting the involvement of intracellular Ca^{2+} stores (Figure 8.). Therefore, we speculate that CFBE41o− cells possess G-protein coupled divalent cation-sensing receptors. We used the ATP "scavengers" hexokinase and apyrase to investigate whether ATP release during experimental procedure could contribute to Zn^{2+}-induced Ca^{2+} signal. Simultaneous application of hexokinase (5 U/ml) and apyrase (1 U/ml) did not prevent effects of Zn^{2+} (Zn^{2+}-induced max. fluorescence = 506 ± 47%, n = 3 vs. Zn^{2+}- induced max. fluorescence $_{\text{hexokinase+apyrase}}$= 545 ± 61%, n = 3, n.s.). Therefore, we concluded that ATP was not involved in Zn^{2+}-induced Ca^{2+} signal. In our experiments external Na^+ prevented changes of $[Ca^{2+}]_i$ caused by heavy metal cations. In

DOI:10.14753/SE.2024.3008

order to investigate that extracellular Na^+ specifically inhibits divalent cation-induced Ca^{2+} signal, we administered Zn^{2+} in a LiCl-rich solution (Na^+-free environment). Under these conditions Zn^{2+} induced an increase in $[Ca^{2+}]_i$ (baseline fluorescence = 95 ± 6%, n = 3, vs. Zn^{2+}-induced fluorescence = 226 ± 31%, n = 3, $p < 0.05$).

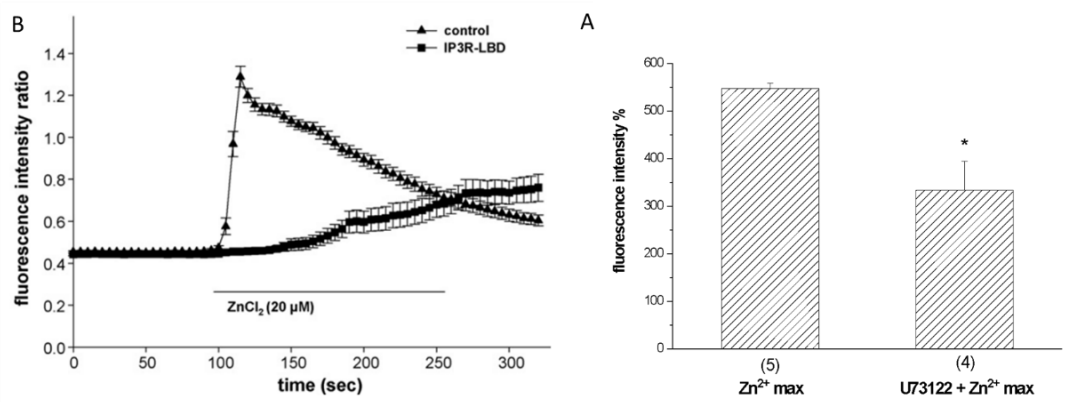

Figure 7. Zn^{2+} -induced Ca^{2+} release from the internal stores is inhibited by blocking PLC and buffering IP_3. (A) Columns represent the maximum of fluorescence intensity % after $ZnCl_2$ (20 µM) was added in the absence (n=5) or presence (n = 4) of the PLC blocker, U73122 * vs. Zn^{2+} max ($p < 0.05$). A single coverslip contained at least 20 cells. (B) The N-terminal IP_3 binding region of the type-I IP_3 R was fused to the monomeric red fluorescent protein (mRFP) for expression in CFBE cells. Fusion of these domains to fluorescent proteins allowed monitoring both the expression levels and the localization of the proteins simultaneously with cytoplasmic Ca^{2+} measurements. In cells expressing this domain Ca^{2+} response evoked by Zn^{2+} was reduced (n = 9, 18 cells) compared the non-expressing control cells (n = 9, 18 cells) indicating the involvement of the IP_3 second messenger pathway in the process.

Based on figure from Hargitai D, Pataki A, Raffai G, Füzi M, Dankó T, Csernoch L, Várnai P, Szigeti GP, Zsembery A. Calcium entry is regulated by Zn^{2+} in relation to extracellular ionic environment in human airway epithelial cells. Respir. Physiol. Neurobiol. 2010 Jan 31;170(1):67-75.

DOI:10.14753/SE.2024.3008

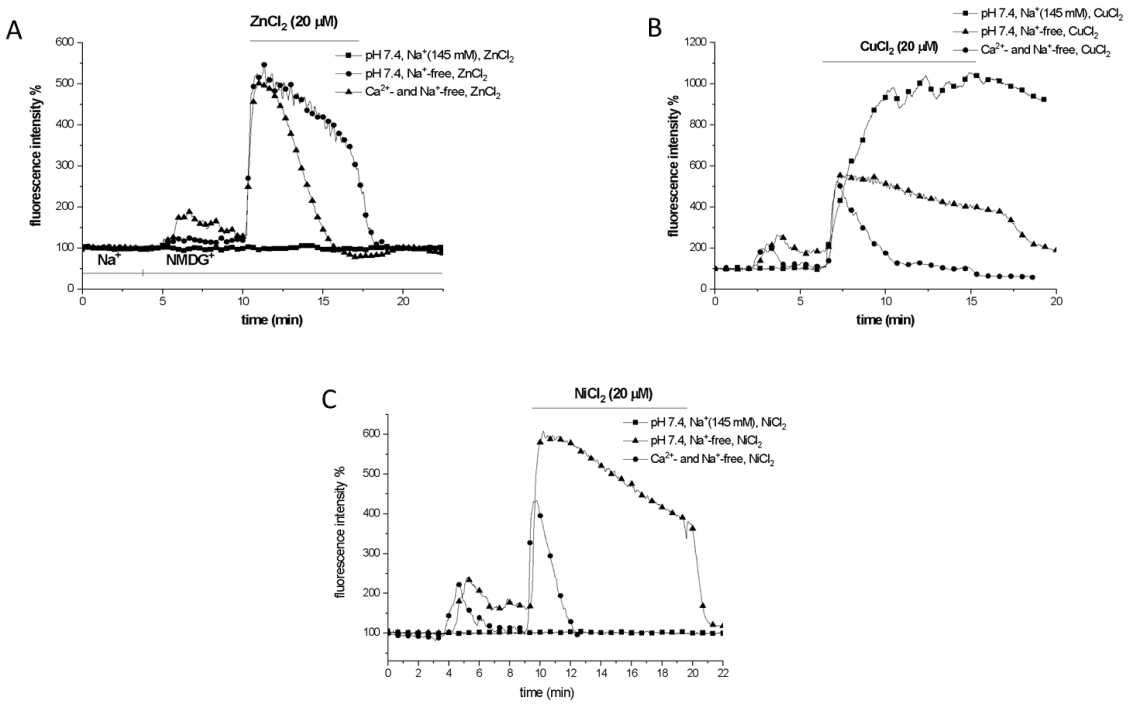

Figure 8. Effects of Zn^{2+}, Ni^{2+} and Cu^{2+} on $[Ca^{2+}]_i$ in Na^+ -containing and Na^+ -free external solution. (A) Original traces showing changes in intracellular Ca^{2+} -level following administration of $ZnCl_2$ (20 μM) at pH 7.4 in presence of physiologic and absence of extracellular Ca^{2+} and/or Na^+. Na^+ was replaced with $NMDG^+$. These experiments were performed 4–6 times using cells from at least two different passages with similar results. (B) Original traces showing changes in intracellular Ca^{2+} -level after administration of $NiCl_2$ (20 μM) at pH 7.4 in presence of physiologic and depleted extracellular Ca^{2+} and/or Na^+. Na^+ was replaced with $NMDG^+$. These experiments were performed 4–6 times using cells from at least two different passages with similar results. (C) Original traces showing changes in intracellular Ca^{2+} -level after administration of $CuCl_2$ (20 μM) at pH 7.4 in presence of physiologic and depleted extracellular Ca^{2+} and/or Na^+. Na^+ was replaced with $NMDG^+$. These experiments were performed 4–6 times using cells from at least two different passages with similar results.

Based on figure from Hargitai D, Pataki A, Raffai G, Füzi M, Dankó T, Csernoch L, Várnai P, Szigeti GP, Zsembery A. Calcium entry is regulated by Zn^{2+} in relation to extracellular ionic environment in human airway epithelial cells. Respir. Physiol. Neurobiol. 2010 Jan 31;170(1):67-75.

4.1.4. Effects of suramin on Zn^{2+}-induced sustained Ca^{2+} signal

Rabbit airway ciliated cells express P2X purinergic receptors which are modulated by extracellular Na^{+}[45], also previous studies suggest the co-assembly of P2X4 and P2X6 subtypes on the surface of airway epithelial cells [55]. We used a non-specific purinergic receptor antagonist, suramin, to investigate whether the effects of Zn^{2+} (without ATP) are at least partially mediated by P2XR subtypes. Although suramin is a weak or even ineffective inhibitor of homomeric P2X4, it can still effectively block heteromeric P2X4/6 receptors in low micromolar concentrations [73, 49]. In wt-CFTR expressing cells, suramin (10 μM) significantly reduced the sustained increase of Fluo-3 fluorescence elicited by Zn^{2+} (Zn^{2+}-induced sustained fluorescence = 425 ± 22 %, n = 5 vs. Zn^{2+}-induced sustained $fluorescence_{suramin}$ = 303 ± 17%, n = 3, $p < 0.05$), supporting the hypothesis that P2X receptors are involved in Zn^{2+} induced $[Ca^{2+}]_i$ increase.

4.1.5. Immunoreactivity of P2X4, P2X5 and P2X6 receptor subtypes

Due to the lack of specific agonists and antagonists, our experiments did not distinguish among the P2X receptor subtypes that are possibly involved in ATP and Zn^{2+}-induced Ca^{2+} entry mechanisms. In order to test whether P2X4, P2X5 and/or P2X6 receptors were present in CFBE41o− cells transfected with ΔF-CFTR, we used immunohistochemical techniques. Strong immunohistochemical labeling was detected with the anti-P2X4 and anti-P2X5 as well as anti-P2X6 receptor antibodies. Simultaneous staining of the P2X4/P2X5 and P2X4/P2X6 receptors showed cytoplasmic co-labeling suggesting that these receptor channel subtypes might be involved in Zn^{2+}-induced Ca^{2+} entry (Figure 9., 10.). Similar results were obtained in wt-CFTR transfected cells (data not shown). Figure 11. indicates the probable regulation of P2XRs and other ion channels and receptors involved in Ca^{2+} homeostasis on the surface of CFBE41o- cells based on our results.

DOI:10.14753/SE.2024.3008

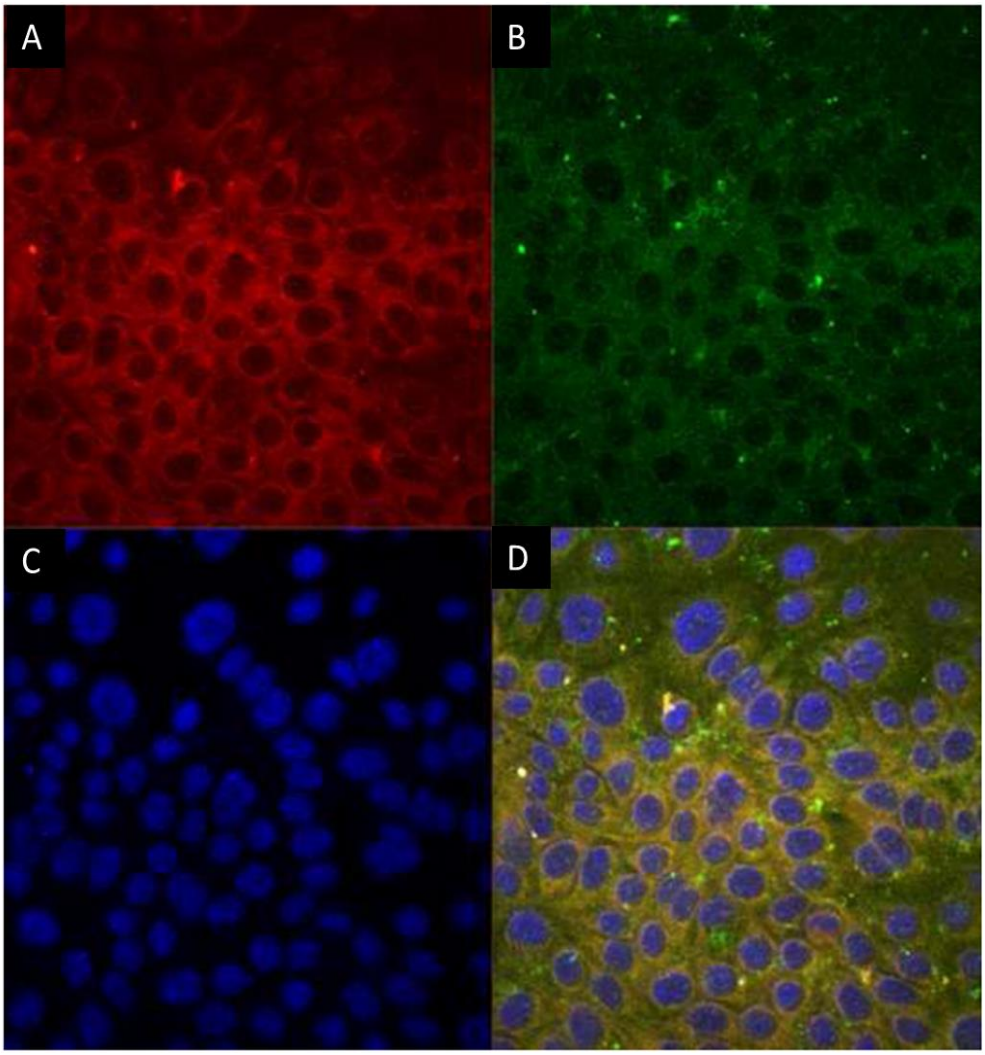

Figure 9. Identification of P2X4 and P2X5 receptor subtypes by immunohistochemistry. (A) Cells were incubated with anti-P2X4 antibodies and stained with TexasRed conjugated bovine anti-rabbit antibodies. (B) Cells were incubated with anti-P2X5 antibodies and stained with FITC conjugated donkey anti-goat antibodies. (C) Only the nucleus was stained. (D) Double staining suggests cytoplasmic co-labeling of P2X4 and P2X5 receptors.

Based on figure from Hargitai D, Pataki A, Raffai G, Füzi M, Dankó T, Csernoch L, Várnai P, Szigeti GP, Zsembery A. Calcium entry is regulated by Zn^{2+} in relation to extracellular ionic environment in human airway epithelial cells. Respir. Physiol. Neurobiol. 2010 Jan 31;170(1):67-75.

DOI:10.14753/SE.2024.3008

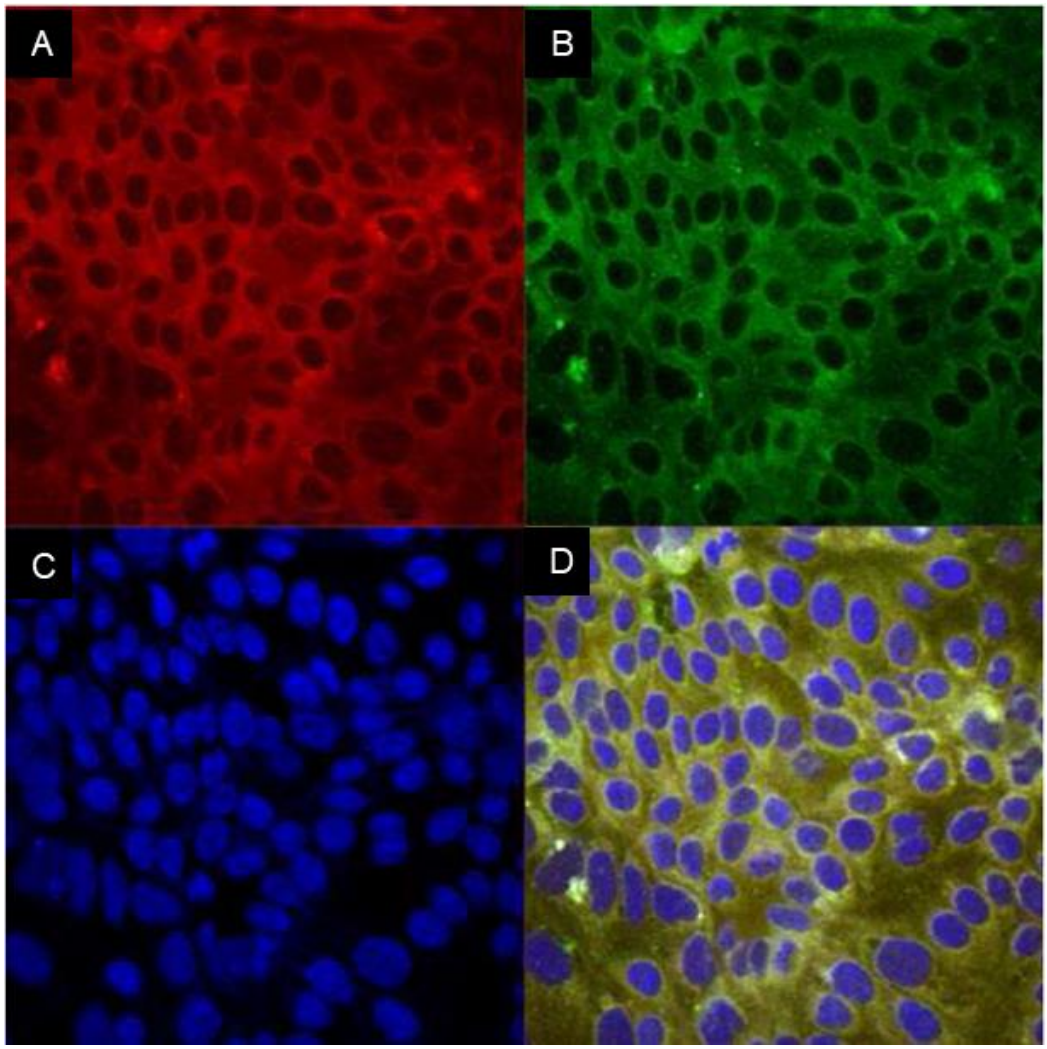

Figure 10. Identification of P2X4 and P2X6 receptor subtypes by immunohistochemistry. (A) Cells were incubated with anti-P2X4 antibodies and stained with TexasRed conjugated bovine anti-rabbit antibodies. (B) Cells were incubated with anti-P2X6 antibodies and stained with FITC conjugated donkey anti-goat antibodies. (C) Only the nucleus was stained. (D) Double staining suggests cytoplasmic co-labeling of P2X4 and P2X6 receptors.

Based on figure from Hargitai D, Pataki A, Raffai G, Füzi M, Dankó T, Csernoch L, Várnai P, Szigeti GP, Zsembery A. Calcium entry is regulated by Zn^{2+} in relation to extracellular ionic environment in human airway epithelial cells. Respir. Physiol. Neurobiol. 2010 Jan 31;170(1):67-75.

DOI:10.14753/SE.2024.3008

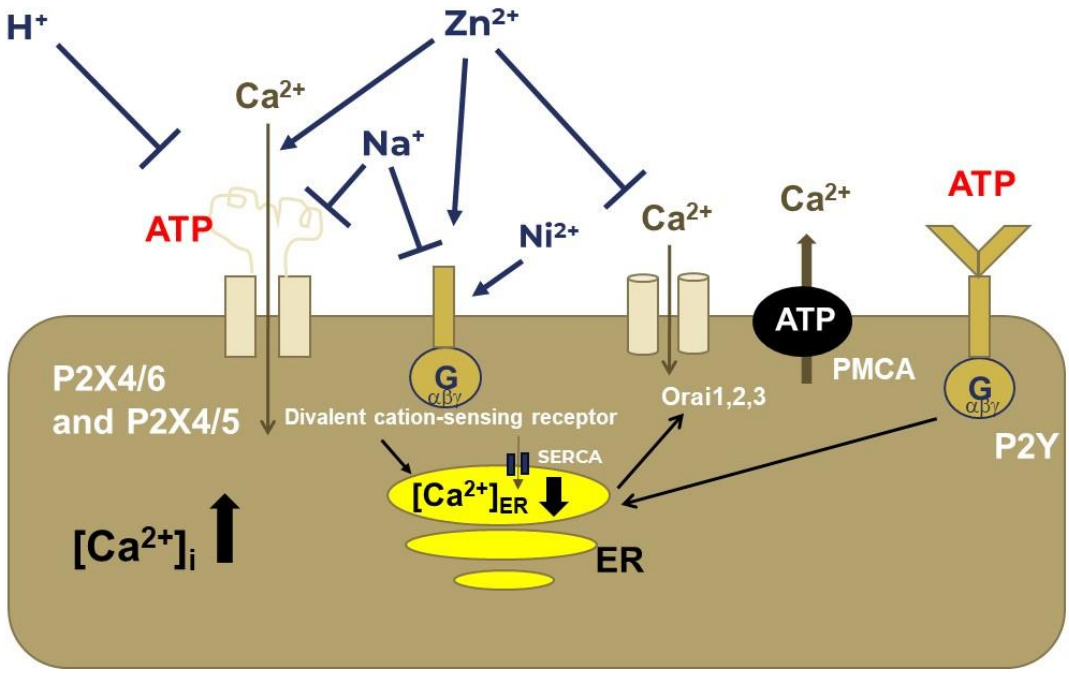

Figure 11. Effect of divalent cations, Na^+, H^+ and ATP on Ca^{2+} signals in CFBE41o- cells based on our results. These epithelial cells carry probably heterodimers of P2X4/5 and P2X4/6 receptors. These P2XR subtypes are inhibited by H^+ and Na^+, while Zn^{2+} further increases the ATP induced sustained Ca^{2+} signal in the absence of Na^+. In the presence on Na^+ the sustained phase of ATP induced Ca^{2+} signal is inhibited by Zn^{2+} which is due to the inhibitory effect of Zn^{2+} on store-operated Ca^{2+} channels (Orai 1,2,3). Zn^{2+} alone (along with other divalent cations, such as Ni^{2+}) also induces $[Ca^{2+}]_i$ increase via a G-protein coupled divalent cation sensing receptor. This receptor is probably also inhibited by extracellular Na^+.

4.2. Safety and efficacy of chronic hypertonic bicarbonate inhalation in a COPD animal model

4.2.1. Long-term $NaHCO_3$ inhalation improves some CSE-induced transient respiratory alterations

Airway function was measured by unrestrained whole-body plethysmography at the beginning and at the end of week 2, 4, 6 and 8. In response to CSE we observed only transient and mild significant alterations in frequency, peak inspiratory flow, inspiratory

and expiratory times throughout the 8-week-long experimental protocol. Compared to the non-smoking respective controls at the end of week 4, frequency and peak inspiratory flow significantly decreased, while inspiratory time increased in the 8.4 % NaCl + CSE-treated group. These alterations were counteracted by 8.4 % $NaHCO_3$ treatment in CSE animals. Further results suggested that $NaHCO_3$ had a protective effect because no significant differences were noted in any parameters of the $NaHCO_3$ + CSE-treated guinea pigs in comparison with the respective controls. Also, compared to the NaCl + CSE animals at weeks 2 and 6, the inspiratory and expiratory times were significantly shorter in the $NaHCO_3$ + CSE group. No changes were revealed in peak expiratory flow, tidal volume and baseline enhanced pause in any groups. We did not observe any alteration in the parameters of different experimental groups at the end of the treatment. The parameters were similar to intact conditions, however it is important to note that long-term hypertonic $NaHCO_3$ aerosol inhalation did not promote any respiratory functional deteriorations in the experimental groups.

4.2.2. Histopathological changes

In the non-smoking or CS-exposed groups quantified by the Case Viewer software (3DHISTECH Ltd, Hungary), there was no decreased airway intraluminal perimeter. Chronic hypertonic $NaHCO_3$ inhalation did not provoked inflammatory response as no significant eosinophil or neutrophil granulocyte infiltration was measured in the non-cartilaginous airways, vessels and septa of the lung. We observed some scattered lymphoid follicles in the lung sections of NaCl -, NaCl + CSE -, as well as $NaHCO_3$-treated guinea pigs (Figure 12., 13.).

DOI:10.14753/SE.2024.3008

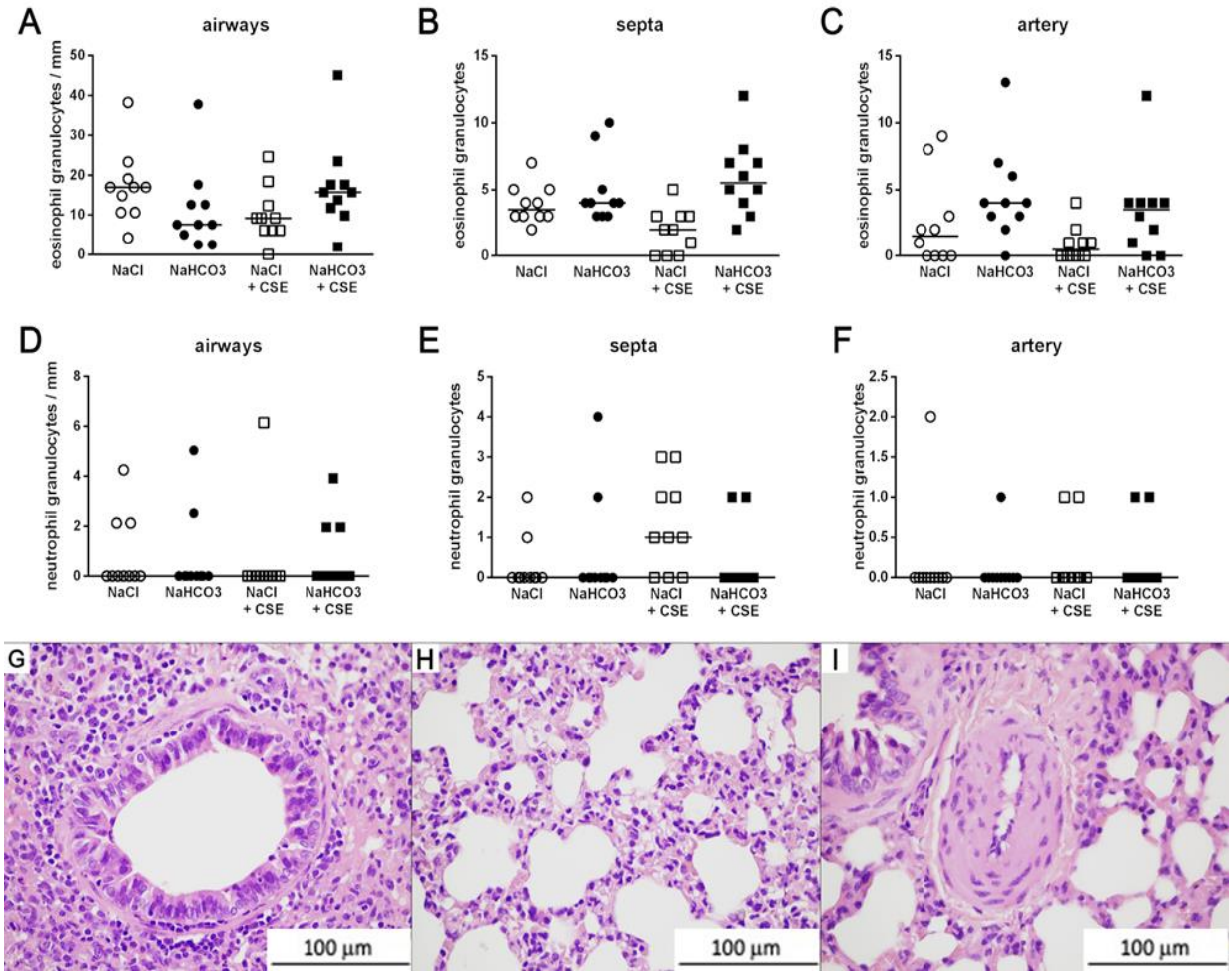

Figure 12. Histopathological assessment of inflammatory cells in the lung. Eosinophil (A-C) and neutrophil (D-F) granulocyte numbers measured in the airways (A, D, G), septa (B, E, H) and vessels (C, F, I). n=10 measurements group, graph represents individual data and median; Kruskal-Wallis, followed by Dunn's multiple comparisons test.

Based on figure from Csekő K, Hargitai D, Draskóczi L, Kéri A, Jaikumpun P, Kerémi B, Helyes Z, Zsembery Á. Safety of chronic hypertonic bicarbonate inhalation in a cigarette smoke-induced airway irritation guinea pig model. BMC Pulm. Med. 2022 Apr 7;22(1):131.

DOI:10.14753/SE.2024.3008

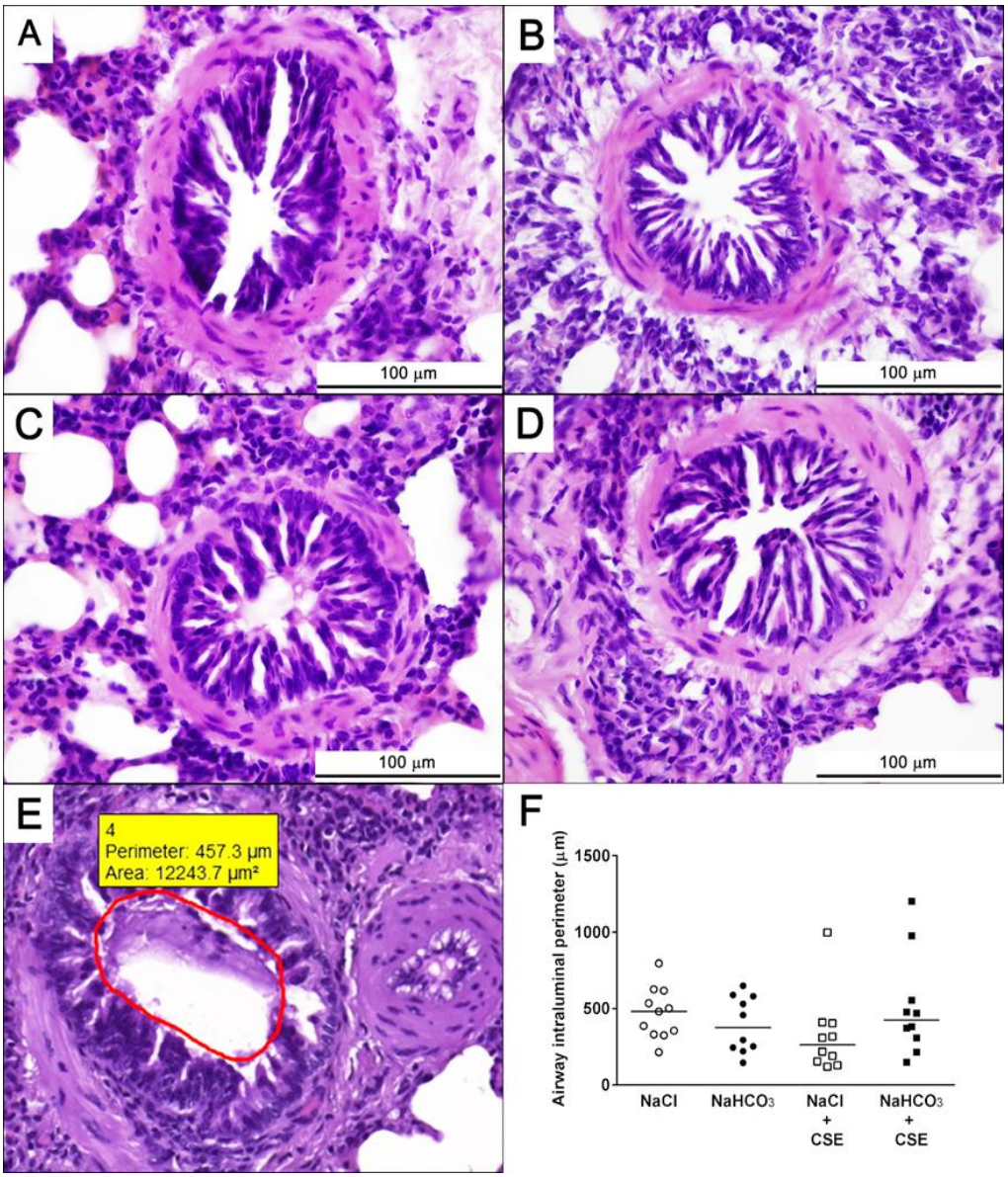

Figure 13. Measurement of airway intraluminal perimeter. Representative histopathological pictures of bronchioles of (A) NaCl, (B) $NaHCO_3$, (C) NaCl + CSE, and (D) $NaHCO_3$ + CSE-treated guinea pigs. Neither treatment induced significant changes in airway intraluminal perimeter (E). n = 10 measurements/group, graph represents individual data and median; Kruskal–Wallis followed by Dunn's multiple comparisons test. Panel (F) represents the method for measurement.

Based on figure from Csekő K, Hargitai D, Draskóczi L, Kéri A, Jaikumpun P, Kerémi B, Helyes Z, Zsembery Á. Safety of chronic hypertonic bicarbonate inhalation in a cigarette smoke-induced airway irritation guinea pig model. BMC Pulm. Med. 2022 Apr 7;22(1):131.

4.2.3. Laboratory parameters

Chronic inhalation of hypertonic $NaHCO_3$ did not induce metabolic alkalosis, because alkaline urine pH is characteristic of herbivores and was within the physiologic range. Electrolyte balance, such as sodium and chloride; creatinine (related to kidney function) and total protein, albumin, bilirubin, alkaline phosphatase, alanine transaminase levels (indicators of liver functions) were also within the normal range. Hyperkalemia observed in all groups might be explained by hemolysis on blood collection. The arterial blood gas analysis performed before tissue harvesting showed acute respiratory acidosis with elevated $PaCO_2$ and low arterial pH is most probably due to respiratory depression induced by pentobarbital anesthesia. Neither hypertonic $NaHCO_3$ treatment, nor CSE affected the body weight gain of animals (Figure 14., Table 2.).

Table 2. Data represent the mean ± SEM of 4 animals / group. $PaCO_2$: partial pressure of carbon dioxide in arterial blood, K^+: potassium ion, Cl^-: chloride anion, Ca^{2+}: calcium ion Normal values based on: The Laboratory Rabbit, Guinea Pig, Hamster, and Other Rodents DOI: 10.1016/B978-0-12-380920-9.00003-1 Page 69., Table 3.7., Bar-Ilan A, Marder J. Acid base status in unanesthetized, unrestrained guinea pigs. Pflugers Arch. 1980 Mar;384(1):93-7. Based on table from Csekő K, Hargitai D, Draskóczi L, Kéri A, Jaikumpun P, Kerémi B, Helyes Z, Zsembery Á. Safety of chronic hypertonic bicarbonate inhalation in a cigarette smoke-induced airway irritation guinea pig model. BMC Pulm Med. 2022 Apr 7;22(1):131.

Parameter	**NaCl**	**$NaHCO_3$**	**NaCl + CSE**	**$NaHCO_3$ + CSE**	**Normal value**
Arterial pH	**7.17**	**7.35** ±0.22	**7.23**	**7.16** ±0.07	**7.44**±0.032
standard HCO_3^- (mmol/l)	**17.1**	**26.9** ±5.85	**19.1**	**18.1** ±1.52	**24.4**±2.8
$PaCO_2$ (mmHg)	**64.3**	**59.5** ±10.45	**59**	**72.83** ±4.61	**91.9**±7.3
K^+ (mmol/l)	**9.19** ±1.15	**8.38** ±1.37	**8.47** ±0.37	**7.48** ±0.77	**4.0-8.0**
Cl^- (mmol/l)	**94.00** ±0.41	**92.25** ±1.93	**96.00** ±0.58	**94.25** ±0.85	**90-115**
Ca^{2+} (mmol/l)	**2.89** ±0.05	**2.66** ±0.07	**2.77** ±0.06	**3.00** ±0.04	**2.4-3.1**

DOI:10.14753/SE.2024.3008

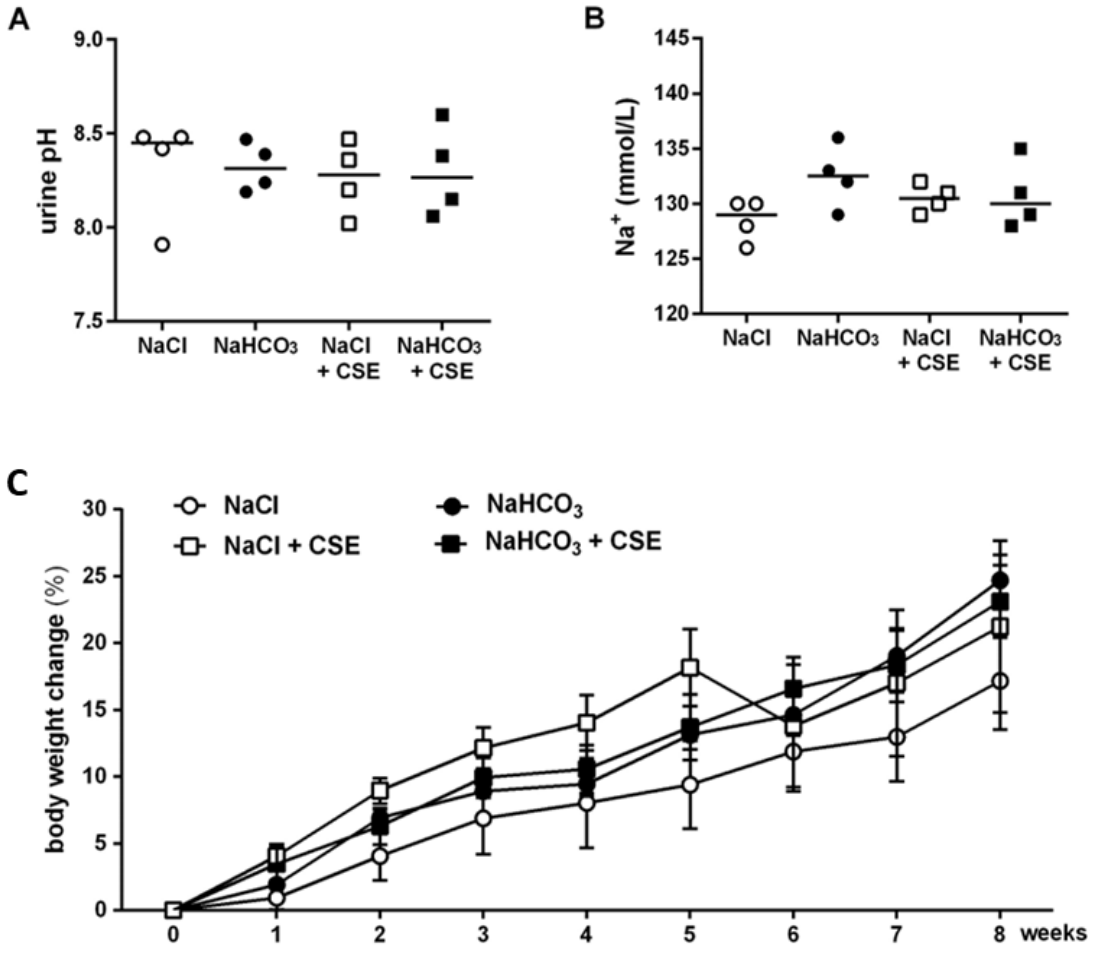

Figure 14. Laboratory parameters and body weight change at the end of the treatment protocol. Urine pH (A), Na^+ (B) levels of guinea pigs 8 weeks after hypertonic HCO_3^- aerosol and chronic cigarette smoke exposure compared to NaCl treatment. Graph represents individual data and median; Kruskal-Wallis followed by Dunn's multiple comparisons test. Panel (C) demonstrates weight change throughout the 8-week-long protocol. Data represent means ± SEM, two-way ANOVA followed by Tukey's multiple comparisons test.

Based on figure from Csekő K, Hargitai D, Draskóczi L, Kéri A, Jaikumpun P, Kerémi B, Helyes Z, Zsembery Á. Safety of chronic hypertonic bicarbonate inhalation in a cigarette smoke-induced airway irritation guinea pig model. BMC Pulm. Med. 2022 Apr 7;22(1):131.

5. Discussion

The role of ATP in energy transfer inside cells is well-recognized. Later ATP revealed to be not merely an energy-carrier molecule [74] but also it is a signaling messenger [41]. Purinergic signaling is known to be important for mucociliary clearance due to enhancing surfactant release, mucin secretion and ciliary beat frequency, also it has effect on smooth muscle situated in the wall of the bronchial tree. Nucleotides are also involved in the activation of the immune system via effect on alveolar macrophages, lung dendritic cells, eosinophils and lung mast cells [75, 76]. Release of ATP from lung epithelial cells was detected with bioluminescence [77]. Nucleotide release provides a mechanism for airway surface liquid homeostasis [78]. Ramsingh et al. [79] proved that cell deformation by surface tension forces near the air-liquid interface causes calcium-dependent ATP-release. This mechanism allows the cells to detect low content of surface liquid or surfactant, leading to ATP release to induce secretion of mucus, fluid and surfactant. Released ATP exerts an autocrine regulation of epithelial sodium absorption by inhibiting ENaC [80]. Released ATP reaches sufficient concentrations in ASL to activate purinergic receptors, such as P2Y2 [81], supporting the hypothesis that this pathway is a physiological mechanism for epithelial cell volume regulation. P2RX1, P2RX4, P2RX7, P2RY1, P2RY11, and P2RY14 were revealed as the most highly expressed purinergic receptors in lung tissue [41]. In CF epithelial cells from multiple tissues, expression of P2X and P2Y purinergic receptors appears unaffected, offering the possibility to target these receptors and activate alternative, calcium-dependent chloride channels via intracellular calcium increase by purinergic receptor activation [47].

Zinc is an indispensable trace metal with a role of catalyzing enzyme actions, also zinc plays a role in regulation of gene expression by binding to extended DNA sequences through bonding to zinc-finger motifs in proteins [82]. Other zinc-containing enzymes are taking part in tissue growth, development, and maintenance of the nervous system. However, there is growing evidence that trace metals, such as zinc are allosteric modulators of certain receptors. For instance, in colonocytes, extracellular Zn^{2+} triggers a rise in cytosolic Ca^{2+} from internal stores by activation of a G_q-coupled Zn^{2+} sensing receptor GPR39 [56, 68, 69]. On the other hand extracellular Zn^{2+} interacts with receptor channels such as NMDA, GABA and P2X purinergic receptors [83, 84, 85, 86]. Zinc is also able to increase ciliary beat frequency in a calcium dependent manner in airway

epithelia [9]. Zinc can either inhibit or activate P2X receptors depending on the expression of receptor subtypes [86, 87]. Furthermore, zinc inhibits SOCs, which is a major Ca^{2+} entry pathway on non-excitable cells [54, 58]. According to the experiments performed by Gore et al., zinc does not permeate SOCs [58], but acts as a competitive inhibitor of calcium influx [88]. Application of dithiothreitol and β-mercaptoethanol completely eliminated the inhibitory effect of zinc, suggesting that cysteines are part of the binding site of Zn^{2+} in human salivary gland cells. In our studies zinc inhibited the plateau phase of ATP-induced calcium entry in CFBE41o$^-$ cells. Also, in different airway epithelial models zinc was found to activate P2XRs and inhibit SOCs. We hypothesized that in our experiments calcium entry was mediated mainly by SOCs. Therefore, we used barium - which is not a substrate of PMCA - because it permeates the same entry pathways as calcium and also increases the Fluo-3 fluorescence [89, 90]. Zinc inhibited barium influx, therefore we concluded that it blocked SOCs rather than potentiated PMCA. This data suggests that zinc reduces the sustained calcium plateau in Na^+ -rich extracellular environment by blocking SOCs. Furthermore, Huidobro-Toro et al. suggest zinc binding to the facilitator site results in allosteric modulation of the receptor, changing the conformation causing an increased conductance for calcium [85].

Zinc further increased ATP induced Ca^{2+} signal following complete substitution of Na^+ with the large organic cation, $NMDG^+$. The ionic composition of the ASL is controversial. Cowley et al. [91] found Na^+ and Cl^- concentrations of 41 mM and 45 mM, respectively. However, analyzing rat trachea and nasal cavity by X-ray microanalysis, Vanthanouvong et al. [92] found slightly higher concentrations of these ions. Therefore, we tested the effects of zinc at different extracellular Na^+ concentrations. According to our experiments, zinc could enhance ATP-induced Ca^{2+} entry at sodium levels lower than 40 mM. Intracellular acidification could follow external Na^+ withdrawal that might also influence cytosolic Ca^{2+} levels.

Our finding that zinc alone was able to induce a biphasic Ca^{2+} signal only in a sodium-free environment confirms the previous observations by Zsembery et al. obtained in IB3-1 airway epithelial cells [54]. Nonetheless, regulation of Zn^{2+}-induced Ca^{2+} signals by external pH differ significantly in CFBE41o− and IB3-1 cells. In CFBE41o− cells the effects of Zn^{2+} were seen at pH 7.4 whereas in IB3-1 cells external alkalinization (pH 7.9) was required to detect an increase in cytosolic Ca^{2+} levels. This phenomenon might be due to different compositions of P2X receptor subtypes expressed in these two CF airway epithelial cell lines. An irreversible inhibitor of the SERCA pump, thapsigargin abolished

the peak of Ca^{2+} signal induced by zinc in IB3-1 cells [54]. As the PLC inhibitor, U73122 partially blocked and IP_3 buffering significantly reduced zinc-induced calcium release from the intracellular stores, we concluded that a G-protein coupled receptor might be involved in zinc mediated Ca^{2+} signal in CFBE41o$^-$ cells. In order to examine the role of P2XR in sustained part of Ca^{2+} signal induced by Zn^{2+} alone, we used suramin, which significantly reduced the sustained phase of Zn^{2+} provoked $[Ca^{2+}]_i$ increase. However, suramin was originally used as an anti-infective agent since the 1920s, it is known to inhibit several enzymes and growth factors. Besides being a non-specific and weak inhibitor of P2 receptors, it also inhibits $GABA_A$ receptors [93] and even CFTR [94], nonetheless, it interacts with the calmodulin domain of the ryanodine receptors [95]. Previous data suggested [55] that not only P2X4 but P2X5 and P2X6 receptors are expressed on the surface of human airway epithelial cells. Although suramin is a conflictingly weak or ineffective inhibitor of P2X4 receptors, when P2X4 is a part of a heteromeric receptor, such as P2X4/6, suramin antagonizes the effect of ATP [49]. Our results of suramin significantly inhibiting the sustained phase of Ca^{2+} signal in CFBE41o- cells further supports the hypothesis that P2XRs might be involved in Zn^{2+} induced $[Ca^{2+}]_i$ increase.

Furthermore, we have demonstrated that Ni^{2+} and Cu^{2+} evoke biphasic Ca^{2+} signals only in a sodium-free environment. Therefore, it is possible that Na^+ occupies the binding site of divalent cations as it has been revealed in calcium sensing receptors [96] and P2XRs [46]. Also Na^+ is able to pass through the extracellular vestibule and the pore of P2XRs, entering the cells via cytoplasmic fenestrations [97]. Thus, it is possible that rather specific zinc-sensing receptors, divalent cation-sensing receptors are involved. The Ca^{2+} signal induced by Zn^{2+} and Ni^{2+} proved to be reversible in Na^+ containing external solution, while Cu^{2+} induced a sustained and irreversible elevation of cytosolic Ca^{2+}. This latter effect was probably due to cell death caused by continuous Na^+ entry. In fact, Yu and Eaton have previously demonstrated that Cu^{2+} stimulated Na^+ entry via ENaCs in A6 kidney epithelial cells [98]. Alkaline pH might potentiate the effect of metal ions because OH^- unmask the binding site of divalent cations [99, 100].

Based on previous studies we speculate that mainly $P2X_4$ receptor subtypes participate in ATP and / or Zn^{2+} induced Ca^{2+} entry [54, 55]. Other experiments proved that $P2X_{cilia}$ receptor channels contain $P2X_4$ receptor subtypes [46]. Furthermore, when measuring RNA content, $P2X_1$, $P2X_4$ and $P2X_7$ proved to be the most highly expressed P2X receptor subtypes in lung and airway tissue [41]. Our immunohistochemical data indicate that

besides $P2X_4$, $P2X_5$ and $P2X_6$ receptors subtypes are present on CFBE41o$^-$ cells. However, determination of P2X receptor subunit composition was beyond the scope of our study. The name “mucoviscidosis” has been completely ignored in favor of “cystic fibrosis”, however the pathophysiology of this disease starts with obstruction of airways, hollow organs and gland ducts by thick mucus. The underlying cause behind CF is a defective anion channel because of mutation in CFTR gene. One may ask why does an anion channel defect cause pathologic mucus secretion? First, it was believed that in CF mucus is abnormally synthetized, but this hypothesis has never been proved by reliable data. Changes in composition of CF mucus are rather due to chronic inflammation and persistent bacterial infection. Organs affected by CF secrete different mucins (e.g. MUC5AC in airway epithelia, MUC5B in submucosal glands, MUC2 in intestine, etc.), with different physical properties, but these products all tend to aggregate and plug lumens. This observation suggests that mucus itself is not abnormal but the manner and condition under which mucins are released could be responsible for these alterations. In fact, it is generally believed that mucus in CF is thick because it is “dehydrated” [19]. On the other hand, it has been reported that sodium and water are hyper-reabsorbed from the airways. This observation could explain alterations in the airways but does not provide explanation to thick mucin in other organs (e.g. pancreas) where fluid absorption does not occur even under physiological circumstances. On the other hand, the hypo-secretion theory assumes that once mucin is secreted, it is without further access to fluid. However, it is not likely, because the vast majority of secreting epithelia is permeable to water, so even when active electrolyte and fluid secretion is compromised, passive water transport is still able to hydrate the mucin on the surface (resulting in lumen dilation). Nonetheless, it seems that both increased reabsorption of sodium and impaired anion (Cl^- and HCO_3^-) secretion as well as consequential intracellular water retention contribute to the thick intraluminal secrete [19]. It has been demonstrated that not only Cl^{--} but HCO_3^- transport is also impaired in CF. How can reduced HCO_3^- secretion lead to the formation of thick mucus? Gel-forming mucin is stored intracellularly in granules where Ca^{2+} and H^+ stabilize them and prevent unfolding. Once secreted, Ca^{2+} and H^+ are removed, and this process is hypothesized to be guided by HCO_3^-, which reacts with these cations. In CF, HCO_3^- concentrations could impair calcium removal and acidify the pH leading to the formation of the mucus plugs [19]. Hypertonic sodium chloride solutions are currently used as mucolytic agents because they increase the driving force for transepithelial water secretion. Sodium bicarbonate has also been considered as a mucolytic agent for decades.

Patients with chronic respiratory disorders instill several OTC (over the counter) inhalation solutions (i.e. spring waters of mineral salts). A common feature of these solutions is the high HCO_3^- concentration (up to approximately 178 mM corresponding to 1,5 %). Intraluminal HCO_3^- is not only useful because it promotes proper mucus unfolding and stabilization in the airways, but also reduces inflammatory responses [101] and enhances bacterial killing capacity of the innate immune system. Also high concentrations of bicarbonate significantly inhibit the growth of *E. coli*, *P. aeruginosa* and *S. aureus*. Bicarbonate also inhibits the biofilm formation of *P. aeruginosa* [102]. Furthermore, HCO_3^- also influences the pH of the ASL via the HCO_3^-/ CO_2 buffer system [102]. These effects directly affect the properties of ASL and the mucociliary clearance.

COPD is a chronic inflammatory response of the airways to environmental elements, mainly cigarette smoke. Although the disease is heterogenous -variable phenotypes exist ranging from chronic bronchitis to emphysema- airflow limitation is associated with all COPD patients. Small airways are affected which results in increased inflammation, smooth muscle hyperplasia, fibrosis, increased number of goblet cells and consequential mucus plugging [**61**, 30]. Thick mucus and recurrent inflammation are common features of COPD and CF, therefore effects of inhaled HCO_3^- are desirable in both diseases. Thus, there is a need to define both the beneficial and harmful effects of chronic HCO_3^- inhalation. Our results showed that 8-week-long inhalation of either hypertonic $NaCO_3$ (8,4 %) or NaCl (8,4 %) does not elicit harmful effects even in cigarette smoke-exposed guinea pig airways, and therefore both may be considered to be equally safe. HCO_3^- even improved some cigarette-induced mild respiratory functional changes compared to hypertonic NaCl (8,4 %) administration: in the 8.4 % NaCl + CSE-treated group frequency and peak inspiratory flow significantly decreased, meanwhile the inspiratory time increased compared to the non-smoking respective controls at the end of week 4. These alterations were counteracted by 8.4 % $NaHCO_3$ treatment in CSE animals. $NaHCO_3$ appeared to be protective because in contrast to the NaCl-treated animals, no significant differences developed in any parameters of the $NaHCO_3$ + CSE-treated guinea pigs in comparison with the respective controls, also the inspiratory and expiratory times were significantly shorter in the $NaHCO_3$ + CSE group compared to the NaCl + CSE animals at weeks 2 and 6. However, these changes were only transient, these data suggests that $NaHCO_3$ is not only safe but also beneficial when applied in aerosols.

In our experimental setup, we chose a cigarette smoke-exposed guinea pig model, because these animals are easy to breed (especially compared to CF ferrets and pigs) and their

lung anatomy and physiology share common features with humans [103]. However, our results could have important implications in CF as well, as both chronic lung diseases share a feature of CFTR dysfunction. Although our primary goal was to investigate the safety of hypertonic $NaCO_3$ inhalation *in vivo*, we are aware of the limitations of these studies. The eight-week long inhalation protocol has not induced significant inflammation in the lungs. Indeed, not exclude the possibility that the lack of inflammation is due to the effect of hypertonic sodium chloride, which masks the cigarette-smoke induced alterations. Hypertonic NaCl (3-7 %) has long been used in the treatment of CF because it is known to improve lung function, because it has been shown to enhance mucociliary clearance [104]. In 2006 the National Hypertonic Saline in Cystic Fibrosis Study Group has been conducted a study for 48 weeks, when 164 CF patients received either hypertonic (7 %) or isotonic (0,9 %) saline in a randomized manner [105]. The forced vital capacity (FVC) and forced expiratory volume in 1 s (FEV_1) showed no significant difference between the two groups, but there was a statistically significant difference in the absolute change in lung function, moreover the frequency of exacerbations reduced in the hypertonic saline group. Nebulized $NaHCO_3$ solution (4,2 %) has been shown to have beneficial short-term effects in patients with "reactive airway dysfunction syndrome" followed by chlorine gas inhalation [106]. Also, bronchoalveolar lavage is proved to be safe and inhibits fungal and bacterial growth in individuals with lower respiratory tract infections [107]. So application of HCO_3^- as an adjuvant might be beneficial along with antimicrobial, antifungal or anti-tuberculosis drugs. HCO_3^- also affects the rheological properties of the sputum reducing its viscosity. HCO_3^- is calcium chelating agent by which it decreases the gel strength of the sputum by helping mucin strands to expand [108]. Recent clinical data indicate that nebulized HCO_3^- inhalation is safe and well-tolerated in patients with CF [109]. These authors have also concluded that administration of HCO_3^- elevated airway pH and reduced sputum viscosity. Our data show that chronic inhalation of hypertonic $NaHCO_3$ (8,4 %) increased neither blood nor urine pH in guinea pigs. Moreover, weight-gains were similar in animals treated with either hypertonic NaCl or $NaHCO_3$ demonstrating that both aerosols were well-tolerated. (However, caution is required when high concentrations of bicarbonate are applied *in vivo*. In vitro measurements by A. Ermund et al. showed that tissue integrity was disrupted when applying $NaHCO_3$ in concentrations higher than 115 mM [36].) Secretion and unfolding of hydrated and viscous mucin in the presence of HCO_3^- is only one requirement for physiological ASL composition and subsequent proper mucociliary clearance in the

airways. The periciliary layer of ASL is also crucial to maintain effective ciliary beat. Ion content of the periciliary layer is regulated by CFTR, Ca^{2+} activated chloride channel (CaCC), chloride channel (CLC) 2 and ENaC. The osmotic gradient generated by these channels results in fluid movement from airspaces to the interstitium that regulates ASL height. Given the CFTR regulated apical chloride secretion and ENaC mediated Na^{+} reabsorption are crucial in maintaining the homeostasis of the periciliary layer, it is not surprising that these two channel activities need to be balanced. This is supported by the observation that airway epithelia of CF patients have elevated amiloride-sensitive Na^{+} reabsorption, demonstrating that CFTR regulates ENaC activity [110]. The mechanism of cross-talk between CFTR and ENaC is further complicated by the fact that CFTR activity and ENaC function are regulated by similar physiological (β-agonists) and environmental factors, such as hypoxia, inflammatory responses and oxidative stress. In CF and COPD the activity of CFTR is impaired [111], therefore stimulation of alternative anion channels, including CaCCs could improve the mucociliary clearance [29].

Previous data suggest that at least two pathways exist for epithelial Cl^{-} and HCO_3^{-} secretion; one dependent on CFTR and another dependent on CaCC [112]. Failure to secrete HCO_3^{-} likely results poor mucociliary and pathogen clearance in CF airways. CaCCs are regulated by intracellular Ca^{2+} concentration, thus increasing Ca^{2+} level via purinergic receptors is necessary for these channels to secrete both chloride and bicarbonate ions. However, prolonged increment of $[Ca2^{+}]_i$ can also result in cell death, previous results indicate that ATP and Zn^{2+} induced Ca^{2+} signals are reversible and provoke a significant Cl^{-} secretion response in CF and non-CF mouse nasal epithelium *in vivo*. This effect was reversible and reproducible upon removal and re-addition of ATP and Zn^{2+} [54]. Thus, CaCCs should be seen as a target for therapy in CF and possibly other airway diseases such as COPD.

DOI:10.14753/SE.2024.3008

6. Conclusions

Investigating the calcium homeostasis of human airway epithelial cells *in vitro* and studying the effects of inhalation of hypertonic $NaHCO_3$ *in vivo*, I obtained the following results: (i) the parallel removal of Na^+ and alkalinization of the extracellular environment significantly enhanced both the amplitude and duration of ATP-induced Ca^{2+} signal in human airway epithelial cells independent of CFTR protein expression, (ii) Zn^{2+} either potentiates or inhibits ATP-induced Ca^{2+} entry from the extracellular space depending on the absence or presence of extracellular Na^+, (iii) Zn^{2+} and other heavy metal cations stimulate release of Ca^{2+} from internal stores via the PLC-dependent pathway only in Na^+-free environment, (iv) there are multiple subtypes of P2X receptor channels on human airway epithelial cells which might be involved in the divalent metal cation-induced Ca^{2+} entry mechanisms, (v) 8-week-long inhalation of hypertonic $NaHCO_3$ is as safe as NaCl in cigarette smoke-induced airway irritation guinea pig model. HCO_3^- even improved some cigarette-induced mild respiratory functional changes compared to hypertonic NaCl (8,4 %) administration.

These findings indicate that purinergic agonists applied to the airways in an aerosol containing HCO_3^- and Zn^{2+} with low Na^+ concentration (40 mM or less) should be considered potentially valuable therapeutic approach in chronic inflammatory airway diseases such as CF and COPD.

Taken together, data presented here underline the importance of aerosol composition that could further potentiate the efficacy of purinergic agonists.

DOI:10.14753/SE.2024.3008

7. Summary

Among chronic lung diseases CF and COPD have different etiological backgrounds, however impairment of CFTR function is a common phenomenon. Without proper CFTR protein function Cl^- and HCO_3^- secretion is insufficient, while intracellular Na^+ concentration is also elevated due to the lack of ENaC inhibition. The consequence is a thick, sticky mucus covering the airways, resulting in chronic inflammation and airway destruction.

One of the therapeutic approaches for defective CFTR function is the activation of alternative anion channels, such as the Ca-activated chloride channel in the airway epithelium. In our study on epithelial cells we found that parallel removal of Na^+ and alkalinization of the extracellular environment significantly enhanced both the amplitude and duration of ATP-induced Ca^{2+} signal in human airway epithelial cells independent of CFTR protein expression. Zn^{2+} either potentiates or inhibits ATP-induced Ca^{2+} entry from the extracellular space depending on the absence or presence of extracellular Na^+. Zn^{2+} and other heavy metal cations stimulate release of Ca^{2+} from internal stores via the PLC-dependent pathway only in Na^+-free environment. Also, we have found that there are multiple subtypes of P2X receptor channels on airway epithelial cells which might be involved in the divalent metal cation-induced Ca^{2+} entry mechanisms. Compromised HCO_3^- secretion results in thick mucus, therefore we hypothesized that HCO_3^- containing aerosols could be beneficial for patients with CFTR dysfunctions. We have demonstrated that 8-week-long inhalation of hypertonic $NaHCO_3$ is as safe as NaCl in cigarette smoke-induced airway irritation guinea pig model, moreover HCO_3^- even improved some cigarette-induced mild respiratory functional changes. HCO_3^- should be considered a potentially valuable therapeutic agent in chronic inflammatory airway diseases.

We have concluded that in chronic lung diseases with impaired CFTR function the aerosol composition in which a purinergic agonist, is applied is also important, and other additional contents, such as HCO_3^- and Zn^{2+}, can further improve ASL rehydration and mucociliary clearance.

8. References

1. Hanssens LS, Duchateau J, Casimir GJ. CFTR Protein: Not Just a Chloride Channel? Cells. 2021 Oct 22;10(11):2844.
2. Quinton PM. The neglected ion: HCO3-. Nat Med. 2001 Mar;7(3):292-293.
3. Haq IJ, Gray MA, Garnett JP, Ward C, Brodlie M. Airway surface liquid homeostasis in cystic fibrosis: pathophysiology and therapeutic targets. Thorax. 2016 Mar;71(3):284-287.
4. Carattino MD, Mueller GM, Palmer LG, Frindt G, Rued AC, Hughey RP, Kleyman TR. Prostasin interacts with the epithelial Na+ channel and facilitates cleavage of the γ-subunit by a second protease. Am J Physiol Renal Physiol. 2014 Nov 1;307(9):F1080-1087.
5. Saint-Criq V, Gray MA. Role of CFTR in epithelial physiology. Cell Mol Life Sci. 2017 Jan;74(1):93-115.
6. Lu M, Leng Q, Egan ME, Caplan MJ, Boulpaep EL, Giebisch GH, Hebert SC. CFTR is required for PKA-regulated ATP sensitivity of Kir1.1 potassium channels in mouse kidney. J Clin Invest. 2006 Mar;116(3):797-807.
7. Zhang S, Shrestha CL, Wisniewski BL, Pham H, Hou X, Li W, Dong Y, Kopp BT. Consequences of CRISPR-Cas9-Mediated CFTR Knockout in Human Macrophages. Front Immunol. 2020 Aug 18;11:1871.
8. Widdicombe JH. Regulation of the depth and composition of airway surface liquid. J Anat. 2002 Oct;201(4):313-318.
9. Woodworth BA, Zhang S, Tamashiro E, Bhargave G, Palmer JN, Cohen NA. Zinc increases ciliary beat frequency in a calcium-dependent manner. Am J Rhinol Allergy. 2010 Jan-Feb;24(1):6-10.
10. Veit G, Avramescu RG, Chiang AN, Houck SA, Cai Z, Peters KW, Hong JS, Pollard HB, Guggino WB, Balch WE, Skach WR, Cutting GR, Frizzell RA, Sheppard DN, Cyr DM, Sorscher EJ, Brodsky JL, Lukacs GL. From CFTR biology toward combinatorial pharmacotherapy: expanded classification of cystic fibrosis mutations. Mol Biol Cell. 2016 Feb 1;27(3):424-433.
11. Lubamba B, Dhooghe B, Noel S, Leal T. Cystic fibrosis: insight into CFTR pathophysiology and pharmacotherapy. Clin Biochem. 2012 Oct;45(15):1132-1144.

12. Yu, E., & Sharma, S. Cystic Fibrosis. In *StatPearls*. StatPearls Publishing. [Internet] 2022 [updated 2022; cited 2023 Febr 4] Available from https://www.ncbi.nlm.nih.gov/books/NBK493206/
13. Cystic Fibrosis Foundation: Sweat Test [Internet] 2022 [updated 2022; cited 2023 Jan 6] Available from https://www.cff.org/intro-cf/sweat-test
14. Felton E, Burrell A, Chaney H, Sami I, Koumbourlis AC, Freishtat RJ, Crandall KA, Hahn A. Inflammation in children with cystic fibrosis: contribution of bacterial production of long-chain fatty acids. Pediatr Res. 2021 Jul;90(1):99-108.
15. Garland AL, Walton WG, Coakley RD, Tan CD, Gilmore RC, Hobbs CA, Tripathy A, Clunes LA, Bencharit S, Stutts MJ, Betts L, Redinbo MR, Tarran R. Molecular basis for pH-dependent mucosal dehydration in cystic fibrosis airways. Proc Natl Acad Sci U S A. 2013 Oct 1;110(40):15973-15978.
16. Pezzulo AA, Tang XX, Hoegger MJ, Abou Alaiwa MH, Ramachandran S, Moninger TO, Karp PH, Wohlford-Lenane CL, Haagsman HP, van Eijk M, Bánfi B, Horswill AR, Stoltz DA, McCray PB Jr, Welsh MJ, Zabner J. Reduced airway surface pH impairs bacterial killing in the porcine cystic fibrosis lung. Nature. 2012 Jul 4;487(7405):109-113.
17. Yang N, Garcia MA, Quinton PM. Normal mucus formation requires cAMP-dependent HCO3- secretion and Ca^{2+}-mediated mucin exocytosis. J Physiol. 2013 Sep 15;591(18):4581-4593.
18. Borowitz D. CFTR, bicarbonate, and the pathophysiology of cystic fibrosis. Pediatr Pulmonol. 2015 Oct;50 Suppl 40:S24-S30.
19. Quinton PM. Cystic fibrosis: impaired bicarbonate secretion and mucoviscidosis. Lancet. 2008 Aug 2;372(9636):415-417.
20. World Health Organization. Chronic Obstructive Pulmonary Disease (COPD) [Internet] 2022 [updated 2022 May 20; cited 2023 Febr 4] Available from https://www.who.int/news-room/fact-sheets/detail/chronic-obstructive-pulmonary-disease-(copd)
21. Rab A, Rowe SM, Raju SV, Bebok Z, Matalon S, Collawn JF. Cigarette smoke and CFTR: implications in the pathogenesis of COPD. Am J Physiol Lung Cell Mol Physiol. 2013 Oct 15;305(8):L530-541.
22. Cantin AM, Hanrahan JW, Bilodeau G, Ellis L, Dupuis A, Liao J, Zielenski J, Durie P. Cystic fibrosis transmembrane conductance regulator function is

suppressed in cigarette smokers. Am J Respir Crit Care Med. 2006 May 15;173(10):1139-1144.

23. Dransfield MT, Wilhelm AM, Flanagan B, Courville C, Tidwell SL, Raju SV, Gaggar A, Steele C, Tang LP, Liu B, Rowe SM. Acquired cystic fibrosis transmembrane conductance regulator dysfunction in the lower airways in COPD. Chest. 2013 Aug;144(2):498-506.
24. Sloane PA, Shastry S, Wilhelm A, Courville C, Tang LP, Backer K, Levin E, Raju SV, Li Y, Mazur M, Byan-Parker S, Grizzle W, Sorscher EJ, Dransfield MT, Rowe SM. A pharmacologic approach to acquired cystic fibrosis transmembrane conductance regulator dysfunction in smoking related lung disease. PLoS One. 2012;7(6):e39809.
25. Clunes LA, Davies CM, Coakley RD, Aleksandrov AA, Henderson AG, Zeman KL, Worthington EN, Gentzsch M, Kreda SM, Cholon D, Bennett WD, Riordan JR, Boucher RC, Tarran R. Cigarette smoke exposure induces CFTR internalization and insolubility, leading to airway surface liquid dehydration. FASEB J. 2012 Feb;26(2):533-545.
26. Raju SV, Jackson PL, Courville CA, McNicholas CM, Sloane PA, Sabbatini G, Tidwell S, Tang LP, Liu B, Fortenberry JA, Jones CW, Boydston JA, Clancy JP, Bowen LE, Accurso FJ, Blalock JE, Dransfield MT, Rowe SM. Cigarette smoke induces systemic defects in cystic fibrosis transmembrane conductance regulator function. Am J Respir Crit Care Med. 2013 Dec 1;188(11):1321-1330.
27. Hassan F, Xu X, Nuovo G, Killilea DW, Tyrrell J, Da Tan C, Tarran R, Diaz P, Jee J, Knoell D, Boyaka PN, Cormet-Boyaka E. Accumulation of metals in GOLD4 COPD lungs is associated with decreased CFTR levels. Respir Res. 2014 Jun 23;15(1):69.
28. Raju SV, Lin VY, Liu L, McNicholas CM, Karki S, Sloane PA, Tang L, Jackson PL, Wang W, Wilson L, Macon KJ, Mazur M, Kappes JC, DeLucas LJ, Barnes S, Kirk K, Tearney GJ, Rowe SM. The Cystic Fibrosis Transmembrane Conductance Regulator Potentiator Ivacaftor Augments Mucociliary Clearance Abrogating Cystic Fibrosis Transmembrane Conductance Regulator Inhibition by Cigarette Smoke. Am J Respir Cell Mol Biol. 2017 Jan;56(1):99-108.
29. Bartoszewski R, Matalon S, Collawn JF. Ion channels of the lung and their role in disease pathogenesis. Am J Physiol Lung Cell Mol Physiol. 2017 Nov 1;313(5):L859-L872.

30. Dransfield M, Rowe S, Vogelmeier CF, Wedzicha J, Criner GJ, Han MK, Martinez FJ, Calverley P. Cystic Fibrosis Transmembrane Conductance Regulator: Roles in Chronic Obstructive Pulmonary Disease. Am J Respir Crit Care Med. 2022 Mar 15;205(6):631-640.
31. Åstrand AB, Hemmerling M, Root J, Wingren C, Pesic J, Johansson E, Garland AL, Ghosh A, Tarran R. Linking increased airway hydration, ciliary beating, and mucociliary clearance through ENaC inhibition. Am J Physiol Lung Cell Mol Physiol. 2015 Jan 1;308(1):L22-32.
32. Morrison CB, Markovetz MR, Ehre C. Mucus, mucins, and cystic fibrosis. Pediatr Pulmonol. 2019 Nov;54 Suppl 3(Suppl 3):S84-S96.
33. Anzueto A, Jubran A, Ohar JA, Piquette CA, Rennard SI, Colice G, Pattishall EN, Barrett J, Engle M, Perret KA, Rubin BK. Effects of aerosolized surfactant in patients with stable chronic bronchitis: a prospective randomized controlled trial. JAMA. 1997 Nov 5;278(17):1426-1431.
34. Griese M, Bufler P, Teller J, Reinhardt D. Nebulization of a bovine surfactant in cystic fibrosis: a pilot study. Eur Respir J. 1997 Sep;10(9):1989-1994.
35. Tarrant BJ, Maitre CL, Romero L, Steward R, Button BM, Thompson BR, Holland AE. Mucoactive agents for adults with acute lung conditions: A systematic review. Heart Lung. 2019 Mar-Apr;48(2):141-147.
36. Ermund A, Meiss LN, Gustafsson JK, Hansson GC. Hyper-osmolarity and calcium chelation: Effects on cystic fibrosis mucus. Eur J Pharmacol. 2015 Oct 5;764:109-117.
37. Donaldson SH, Bennett WD, Zeman K, et al. A First in Class Mucus Conditioning Drug - Effect of an Inhaled Alginate Oligosaccharide (Oligo-G) on Mucus Clearance in Subjects with Cystic Fibrosis. In: NACFC, 18-20 Oct 2018, Denver, Colorado, USA Vol 52 2017:S305–S305
38. Sesma JI, Wu B, Stuhlmiller TJ, Scott DW. SPX-101 is stable in and retains function after exposure to cystic fibrosis sputum. J Cyst Fibros. 2019 Mar;18(2):244-250.
39. Danahay HL, Lilley S, Fox R, Charlton H, Sabater J, Button B, McCarthy C, Collingwood SP, Gosling M. TMEM16A Potentiation: A Novel Therapeutic Approach for the Treatment of Cystic Fibrosis. Am J Respir Crit Care Med. 2020 Apr 15;201(8):946-954.

40. Burnstock G. Cell membrane receptors for drugs and hormones: a multidisciplinary approach. New York: Raven. 1978:107-118.
41. Thompson RJ, Sayers I, Kuokkanen K, Hall IP. Purinergic Receptors in the Airways: Potential Therapeutic Targets for Asthma? Front Allergy. 2021 May 31;2:677677.
42. Otero M, Garrad RC, Velázquez B, Hernández-Pérez MG, Camden JM, Erb L, Clarke LL, Turner JT, Weisman GA, González FA. Mechanisms of agonist-dependent and -independent desensitization of a recombinant P2Y2 nucleotide receptor. Mol Cell Biochem. 2000 Feb;205(1-2):115-123.
43. Stoop R, Surprenant A, North RA. Different sensitivities to pH of ATP-induced currents at four cloned P2X receptors. J Neurophysiol. 1997 Oct;78(4):1837-40.
44. Gerevich Z, Zadori ZS, Köles L, Kopp L, Milius D, Wirkner K, Gyires K, Illes P. Dual effect of acid pH on purinergic P2X3 receptors depends on the histidine 206 residue. J Biol Chem. 2007 Nov 23;282(47):33949-33957.
45. Ma W, Korngreen A, Uzlaner N, Priel Z, Silberberg SD. Extracellular sodium regulates airway ciliary motility by inhibiting a P2X receptor. Nature. 1999 Aug 26;400(6747):894-897.
46. Ma W, Korngreen A, Weil S, Cohen EB, Priel A, Kuzin L, Silberberg SD. Pore properties and pharmacological features of the P2X receptor channel in airway ciliated cells. J Physiol. 2006 Mar 15;571(Pt 3):503-517.
47. Zsembery A, Boyce AT, Liang L, Peti-Peterdi J, Bell PD, Schwiebert EM. Sustained calcium entry through P2X nucleotide receptor channels in human airway epithelial cells. J Biol Chem. 2003 Apr 11;278(15):13398-13408.
48. Negulyaev YA, Markwardt F. Block by extracellular Mg2+ of single human purinergic P2X4 receptor channels expressed in human embryonic kidney cells. Neurosci Lett. 2000 Feb 4;279(3):165-168.
49. Khakh BS, Burnstock G, Kennedy C, King BF, North RA, Séguéla P, Voigt M, Humphrey PP. International union of pharmacology. XXIV. Current status of the nomenclature and properties of P2X receptors and their subunits. Pharmacol Rev. 2001 Mar;53(1):107-118.
50. Chataigneau T, Lemoine D, Grutter T. Exploring the ATP-binding site of P2X receptors. Front Cell Neurosci. 2013 Dec 30;7:273.
51. Jacobson KA, Müller CE. Medicinal chemistry of adenosine, P2Y and P2X receptors. Neuropharmacology. 2016 May;104:31-49.

52. Buell G, Collo G, Rassendren F. P2X receptors: an emerging channel family. Eur J Neurosci. 1996 Oct;8(10):2221-2228.
53. Collo G, North RA, Kawashima E, Merlo-Pich E, Neidhart S, Surprenant A, Buell G. Cloning OF P2X5 and P2X6 receptors and the distribution and properties of an extended family of ATP-gated ion channels. J Neurosci. 1996 Apr 15;16(8):2495-2507.
54. Zsembery A, Fortenberry JA, Liang L, Bebok Z, Tucker TA, Boyce AT, Braunstein GM, Welty E, Bell PD, Sorscher EJ, Clancy JP, Schwiebert EM. Extracellular zinc and ATP restore chloride secretion across cystic fibrosis airway epithelia by triggering calcium entry. J Biol Chem. 2004 Mar 12;279(11):10720-10729.
55. Liang L, Zsembery A, Schwiebert EM. RNA interference targeted to multiple P2X receptor subtypes attenuates zinc-induced calcium entry. Am J Physiol Cell Physiol. 2005 Aug;289(2):C388-396.
56. Hershfinkel M, Moran A, Grossman N, Sekler I. A zinc-sensing receptor triggers the release of intracellular Ca^{2+} and regulates ion transport. Proc Natl Acad Sci U S A. 2001 Sep 25;98(20):11749-11754.
57. Huang J, van Breemen C, Kuo KH, Hove-Madsen L, Tibbits GF. Store-operated Ca2+ entry modulates sarcoplasmic reticulum Ca^{2+} loading in neonatal rabbit cardiac ventricular myocytes. Am J Physiol Cell Physiol. 2006 Jun;290(6):C1572-1582.
58. Gore A, Moran A, Hershfinkel M, Sekler I. Inhibitory mechanism of store-operated Ca^{2+} channels by zinc. J Biol Chem. 2004 Mar 19;279(12):11106-11111.
59. Pranke I, Golec A, Hinzpeter A, Edelman A, Sermet-Gaudelus I. Emerging Therapeutic Approaches for Cystic Fibrosis. From Gene Editing to Personalized Medicine. Front Pharmacol. 2019 Feb 27;10:121.
60. Condren ME, Bradshaw MD. Ivacaftor: a novel gene-based therapeutic approach for cystic fibrosis. J Pediatr Pharmacol Ther. 2013 Jan;18(1):8-13.
61. Grand DL, Gosling M, Baettig U, Bahra P, Bala K, Brocklehurst C, Budd E, Butler R, Cheung AK, Choudhury H, Collingwood SP, Cox B, Danahay H, Edwards L, Everatt B, Glaenzel U, Glotin AL, Groot-Kormelink P, Hall E, Hatto J, Howsham C, Hughes G, King A, Koehler J, Kulkarni S, Lightfoot M, Nicholls I, Page C, Pergl-Wilson G, Popa MO, Robinson R, Rowlands D, Sharp T, Spendiff

M, Stanley E, Steward O, Taylor RJ, Tranter P, Wagner T, Watson H, Williams G, Wright P, Young A, Sandham DA. Discovery of Icenticaftor (QBW251), a Cystic Fibrosis Transmembrane Conductance Regulator Potentiator with Clinical Efficacy in Cystic Fibrosis and Chronic Obstructive Pulmonary Disease. J Med Chem. 2021 Jun 10;64(11):7241-7260.

62. Bebok Z, Collawn JF, Wakefield J, Parker W, Li Y, Varga K, Sorscher EJ, Clancy JP. Failure of cAMP agonists to activate rescued deltaF508 CFTR in CFBE41o- airway epithelial monolayers. J Physiol. 2005 Dec 1;569(Pt 2):601-615.
63. Várnai P, Balla A, Hunyady L, Balla T. Targeted expression of the inositol 1,4,5-trisphosphate receptor (IP3R) ligand-binding domain releases Ca^{2+} via endogenous IP3R channels. Proc Natl Acad Sci U S A. 2005 May 31;102(22):7859-7864.
64. Kemény Á, Csekő K, Szitter I, Varga ZV, Bencsik P, Kiss K, Halmosi R, Deres L, Erős K, Perkecz A, Kereskai L, László T, Kiss T, Ferdinandy P, Helyes Z. Integrative characterization of chronic cigarette smoke-induced cardiopulmonary comorbidities in a mouse model. Environ Pollut. 2017 Oct;229:746-759.
65. Domínguez-Fandos D, Peinado VI, Puig-Pey R, Ferrer E, Musri MM, Ramírez J, Barberà JA. Pulmonary inflammatory reaction and structural changes induced by cigarette smoke exposure in the Guinea pig. COPD. 2012 Aug;9(5):473-484.
66. Jung S, Pfeiffer F, Deitmer JW. Histamine-induced calcium entry in rat cerebellar astrocytes: evidence for capacitative and non-capacitative mechanisms. J Physiol. 2000 Sep 15;527 Pt 3(Pt 3):549-561.
67. Faurskov B, Bjerregaard HF. Evidence for cadmium mobilization of intracellular calcium through a divalent cation receptor in renal distal epithelial A6 cells. Pflugers Arch. 2002 Oct;445(1):40-50.
68. Laitakari A, Liu L, Frimurer TM, Holst B. The Zinc-Sensing Receptor GPR39 in Physiology and as a Pharmacological Target. Int J Mol Sci. 2021 Apr 8;22(8):3872.
69. Hershfinkel M. The Zinc Sensing Receptor, ZnR/GPR39, in Health and Disease. Int J Mol Sci. 2018 Feb 1;19(2):439.
70. Hogstrand C, Verbost PM, Wendelaar Bonga SE. Inhibition of human erythrocyte Ca^{2+}-ATPase by Zn^{2+}. Toxicology. 1999 Apr 15;133(2-3):139-145.
71. Babnigg G, Zagranichnaya T, Wu X, Villereal ML. Differential tyrosine phosphorylation of plasma membrane Ca^{2+}-ATPase and regulation of calcium

pump activity by carbachol and bradykinin. J Biol Chem. 2003 Apr 25;278(17):14872-14882.

72. North RA, Surprenant A. Pharmacology of cloned P2X receptors. Annu Rev Pharmacol Toxicol. 2000;40:563-580.
73. Lê KT, Babinski K, Séguéla P. Central P2X4 and P2X6 channel subunits coassemble into a novel heteromeric ATP receptor. J Neurosci. 1998 Sep 15;18(18):7152-7159.
74. Drury AN, Szent-Györgyi A. The physiological activity of adenine compounds with especial reference to their action upon the mammalian heart. J Physiol. 1929 Nov 25;68(3):213-237.
75. Burnstock G, Brouns I, Adriaensen D, Timmermans JP. Purinergic signaling in the airways. Pharmacol Rev. 2012 Oct;64(4):834-868.
76. Kobayashi T, Soma T, Noguchi T, Nakagome K, Nakamoto H, Kita H, Nagata M. ATP drives eosinophil effector responses through P2 purinergic receptors. Allergol Int. 2015 Sep;64 Suppl(0):S30-36.
77. Taylor AL, Kudlow BA, Marrs KL, Gruenert DC, Guggino WB, Schwiebert EM. Bioluminescence detection of ATP release mechanisms in epithelia. Am J Physiol. 1998 Nov;275(5):C1391-1406.
78. Lazarowski ER, Tarran R, Grubb BR, van Heusden CA, Okada S, Boucher RC. Nucleotide release provides a mechanism for airway surface liquid homeostasis. J Biol Chem. 2004 Aug 27;279(35):36855-36864.
79. Ramsingh R, Grygorczyk A, Solecki A, Cherkaoui LS, Berthiaume Y, Grygorczyk R. Cell deformation at the air-liquid interface induces Ca2+-dependent ATP release from lung epithelial cells. Am J Physiol Lung Cell Mol Physiol. 2011 Apr;300(4):L587-595.
80. Poulsen AN, Klausen TL, Pedersen PS, Willumsen NJ, Frederiksen O. Regulation of ion transport via apical purinergic receptors in intact rabbit airway epithelium. Pflugers Arch. 2005 Jul;450(4):227-235.
81. Okada SF, Nicholas RA, Kreda SM, Lazarowski ER, Boucher RC. Physiological regulation of ATP release at the apical surface of human airway epithelia. J Biol Chem. 2006 Aug 11;281(32):22992-23002.
82. Thompson MW. Regulation of zinc-dependent enzymes by metal carrier proteins. Biometals. 2022 Apr;35(2):187-213.

83. Paoletti P, Ascher P, Neyton J. High-affinity zinc inhibition of NMDA NR1-NR2A receptors. J Neurosci. 1997 Aug 1;17(15):5711-5725.
84. Hosie AM, Dunne EL, Harvey RJ, Smart TG. Zinc-mediated inhibition of GABA(A) receptors: discrete binding sites underlie subtype specificity. Nat Neurosci. 2003 Apr;6(4):362-369.
85. Huidobro-Toro JP, Lorca RA, Coddou C. Trace metals in the brain: allosteric modulators of ligand-gated receptor channels, the case of ATP-gated P2X receptors. Eur Biophys J. 2008 Mar;37(3):301-314.
86. Peralta FA, Huidobro-Toro JP. Zinc as Allosteric Ion Channel Modulator: Ionotropic Receptors as Metalloproteins. Int J Mol Sci. 2016 Jul 2;17(7):1059.
87. North RA. Molecular physiology of P2X receptors. Physiol Rev. 2002 Oct;82(4):1013-1067.
88. Cheng P, Tian X, Tang W, Cheng J, Bao J, Wang H, Zheng S, Wang Y, Wei X, Chen T, Feng H, Xue T, Goda K, He H. Direct control of store-operated calcium channels by ultrafast laser. Cell Res. 2021 Jul;31(7):758-772.
89. Okamoto Y, Furuno T, Hamano T, Nakanishi M. Confocal fluorescence microscopy for studying thapsigargin-induced bivalent-cation entry into B cells. Biochem J. 1995 Feb 1;305 (Pt 3)(Pt 3):1011-1015.
90. Ferreira-Gomes MS, Mangialavori IC, Ontiveros MQ, Rinaldi DE, Martiarena J, Verstraeten SV, Rossi JPFC. Selectivity of plasma membrane calcium ATPase (PMCA)-mediated extrusion of toxic divalent cations in vitro and in cultured cells. Arch Toxicol. 2018 Jan;92(1):273-288.
91. Cowley EA, Govindaraju K, Lloyd DK, Eidelman DH. Airway surface fluid composition in the rat determined by capillary electrophoresis. Am J Physiol. 1997 Oct;273(4):L895-899.
92. Vanthanouvong V, Kozlova I, Roomans GM. Ionic composition of rat airway surface liquid determined by X-ray microanalysis. Microsc Res Tech. 2005 Sep;68(1):6-12.
93. Luo H, Wood K, Shi FD, Gao F, Chang Y. Suramin is a novel competitive antagonist selective to α1β2γ2 GABAA over ρ1 GABAC receptors. Neuropharmacology. 2018 Oct;141:148-157.
94. Bachmann A, Russ U, Quast U. Potent inhibition of the CFTR chloride channel by suramin. Naunyn Schmiedebergs Arch Pharmacol. 1999 Oct;360(4):473-476.

95. Papineni RV, O'Connell KM, Zhang H, Dirksen RT, Hamilton SL. Suramin interacts with the calmodulin binding site on the ryanodine receptor, RYR1. J Biol Chem. 2002 Dec 20;277(51):49167-49174.
96. Quinn SJ, Kifor O, Trivedi S, Diaz R, Vassilev P, Brown E. Sodium and ionic strength sensing by the calcium receptor. J Biol Chem. 1998 Jul 31;273(31):19579-19586.
97. Oken AC, Krishnamurthy I, Savage JC, Lisi NE, Godsey MH, Mansoor SE. Molecular Pharmacology of P2X Receptors: Exploring Druggable Domains Revealed by Structural Biology. Front Pharmacol. 2022 Jun 17;13:925880.
98. Yu L, Eaton DC, Helms MN. Effect of divalent heavy metals on epithelial Na+ channels in A6 cells. Am J Physiol Renal Physiol. 2007 Jul;293(1):F236-244.
99. Chang W, Shoback D. Extracellular Ca^{2+}-sensing receptors--an overview. Cell Calcium. 2004 Mar;35(3):183-196.
100. Deng X, Xin Y, Miller CL, Hamelberg D, Kirberger M, Moremen KW, Hu J, Yang JJ. Structural Mechanism of Cooperative Regulation of Calcium-Sensing Receptor-Mediated Cellular Signaling. Curr Opin Physiol. 2020 Oct;17:269-277.
101. Ray SC, Baban B, Tucker MA, Seaton AJ, Chang KC, Mannon EC, Sun J, Patel B, Wilson K, Musall JB, Ocasio H, Irsik D, Filosa JA, Sullivan JC, Marshall B, Harris RA, O'Connor PM. Oral NaHCO3 Activates a Splenic Anti-Inflammatory Pathway: Evidence That Cholinergic Signals Are Transmitted via Mesothelial Cells. J Immunol. 2018 May 15;200(10):3568-3586.
102. Dobay O, Laub K, Stercz B, Kéri A, Balázs B, Tóthpál A, Kardos S, Jaikumpun P, Ruksakiet K, Quinton PM, Zsembery Á. Bicarbonate Inhibits Bacterial Growth and Biofilm Formation of Prevalent Cystic Fibrosis Pathogens. Front Microbiol. 2018 Sep 19;9:2245.
103. Ghorani V, Boskabady MH, Khazdair MR, Kianmeher M. Experimental animal models for COPD: a methodological review. Tob Induc Dis. 2017;15(25):1–13.
104. Reeves EP, McCarthy C, McElvaney OJ, Vijayan MS, White MM, Dunlea DM, Pohl K, Lacey N, McElvaney NG. Inhaled hypertonic saline for cystic fibrosis: Reviewing the potential evidence for modulation of neutrophil signalling and function. World J Crit Care Med. 2015 Aug 4;4(3):179-191.
105. Elkins MR, Robinson M, Rose BR, Harbour C, Moriarty CP, Marks GB, Belousova EG, Xuan W, Bye PT; National Hypertonic Saline in Cystic Fibrosis

(NHSCF) Study Group. A controlled trial of long-term inhaled hypertonic saline in patients with cystic fibrosis. N Engl J Med. 2006 Jan 19;354(3):229-240.

106. Aslan S, Kandiş H, Akgun M, Çakir Z, Inandi T, Görgüner M. The effect of nebulized NaHCO3 treatment on "RADS" due to chlorine gas inhalation. Inhalation Toxicol. 2006;18(11):895–900.
107. El Badrawy MK, Elela MA, Yousef AM, et al. Effect of sodium bicarbonate 8.4% on respiratory tract pathogens. Chest Lung Res. 2018;1(1):3-7.
108. Budai-Szűcs M, Berkó S, Kovács A, Jaikumpun P, Ambrus R, Halász A, Szabó-Révész P, Csányi E, Zsembery Á. Rheological effects of hypertonic saline and sodium bicarbonate solutions on cystic fibrosis sputum in vitro. BMC Pulm Med. 2021 Jul 12;21(1):225.
109. Gomez CCS, Parazzi PLF, Clinckspoor KJ, Mauch RM, Pessine FBT, Levy CE, Peixoto AO, Ribeiro MÂGO, Ribeiro AF, Conrad D, Quinton PM, Marson FAL, Ribeiro JD. Safety, Tolerability, and Effects of Sodium Bicarbonate Inhalation in Cystic Fibrosis. Clin Drug Investig. 2020 Feb;40(2):105-117.
110. Ismailov II, Awayda MS, Jovov B, Berdiev BK, Fuller CM, Dedman JR, Kaetzel M, Benos DJ. Regulation of epithelial sodium channels by the cystic fibrosis transmembrane conductance regulator. J Biol Chem. 1996 Mar 1;271(9):4725-4732.
111. Wellmerling JH, Chang SW, Kim E, Osman WH, Boyaka PN, Borchers MT, Cormet-Boyaka E. Reduced expression of the Ion channel CFTR contributes to airspace enlargement as a consequence of aging and in response to cigarette smoke in mice. Respir Res. 2019 Sep 2;20(1):200.
112. Shamsuddin AKM, Quinton PM. Concurrent absorption and secretion of airway surface liquids and bicarbonate secretion in human bronchioles. Am J Physiol Lung Cell Mol Physiol. 2019 May 1;316(5):L953-L960.

DOI:10.14753/SE.2024.3008

9. Bibliography of the candidate's publications

Publication related to the thesis:

1. Hargitai D, Pataki A, Raffai G, Füzi M, Dankó T, Csernoch L, Várnai P, Szigeti GP, Zsembery Á. Calcium entry is regulated by Zn^{2+} in relation to extracellular ionic environment in human airway epithelial cells. Respir Physiol Neurobiol. 2010 Jan 31;170(1):67-75.

2. Csekő K, Hargitai D, Draskóczi L, Kéri A, Jaikumpun P, Kerémi B, Helyes Z, Zsembery Á. Safety of chronic hypertonic bicarbonate inhalation in a cigarette smoke-induced airway irritation guinea pig model. BMC Pulm Med. 2022 Apr 7;22(1):131.

Other publications:

1. Geszti, F ; Hargitai, D ; Lukats, O ; Gyorffy, H ; Toth, J Basalzellkarzinome des periokularen Bereichs [Basal cell carcinoma of the periocular region] Pathologe. 2013; 34:6 pp. 552-557., 6 p.

2. Dankó T, Hargitai D, Pataki A, Hakim H, Molnár M, Zsembery Á. Extracellular alkalinization stimulates calcium-activated chloride conductance in cystic fibrosis human airway epithelial cells. Cell Physiol Biochem. 2011;27(3-4):401-410.

3. Zsembery Á, Hargitai D. Role of Ca^{2+}-activated ion transport in the treatment of cystic fibrosis. Wiener Medizische Wochenschrift. 2008; 158: 19-20 pp. 562-564., 3 p.

DOI:10.14753/SE.2024.3008

10. Acknowledgements

First, I am extremely grateful to my supervisor, Ákos Zsembery for his constant support, feedback, and encouragement during all these years. Also, I am grateful for the help of Ágnes Pataki and Gábor Raffai, my former colleagues. I would like to extend my thanks to Kata Csekő and Zsuzsanna Helyes from Pécs for working together on our previous article. Special thanks to Andras Kiss, my present boss for supporting me writing this thesis. Also, huge thank to my present colleagues who worked even harder while I had the chance to complete this thesis. Finally, I am deeply grateful for my family for their patience and support during this period.